

1       **Recent advances in aptasensors based on graphene and**  
2                                   **graphene-like nanomaterials**

3       Jianfeng Ping<sup>a,†</sup>, Yubin Zhou<sup>a,†</sup>, Yuanyuan Wu<sup>a</sup>, Vladislav Papper<sup>a</sup>, Souhir Boujday<sup>b,c</sup>,  
4                                   Robert S. Marks<sup>d</sup>, Terry W. J. Steele<sup>a,\*</sup>

5       <sup>a</sup> *School of Materials Science & Engineering, College of Engineering, Nanyang*  
6       *Technological University, 50 Nanyang Avenue, Singapore 639798, Singapore*

7       <sup>b</sup> *Sorbonne Universités, UPMC, Univ Paris 6, UMR CNRS 7197, Laboratoire de*  
8       *Réactivité de Surface, F75005 Paris, France*

9       <sup>c</sup> *CNRS, UMR 7197, Laboratoire de Réactivité de Surface, F75005 Paris, France*

10      <sup>d</sup> *Department of Biotechnology Engineering, Faculty of Engineering Sciences, Ben*  
11      *Gurion University of the Negev, P.O. Box 653, Beer Sheva 84105, Israel*

12                                   \* *Corresponding Author. Tel.:65-65927594; fax: 65-67909081.*

13                                   *E-mail address: wjsteele@ntu.edu.sg*

14                                   <sup>†</sup> *These authors contributed equally to this work.*

15

16 **ABSTRACT**

17 Graphene and graphene-like two-dimensional nanomaterials have aroused tremendous  
18 research interest in recent years due to their unique electronic, optical, and mechanical  
19 properties associated with their planar structure. Aptamers have exhibited many  
20 advantages as molecular recognition elements for sensing devices compared to  
21 traditional antibodies. The marriage of two-dimensional nanomaterials and aptamers  
22 has emerged many ingenious aptasensing strategies for applications in the fields of  
23 clinical diagnosis and food safety. This review highlights current advances in the  
24 development and application of two-dimensional nanomaterials-based aptasensors  
25 with the focus on two main signal-transducing mechanisms, i.e. electrochemical and  
26 optical. A special attention is paid to graphene, a one-atom thick layer of graphite with  
27 exceptional properties, representing a fastgrowing field of research. In view of the  
28 unique properties of two-dimensional nanostructures and their inherent advantages of  
29 synthetic aptamers, we expect that high-performance two-dimensional  
30 nanomaterials-based aptasensing devices will find extensive applications in  
31 environmental monitoring, biomedical diagnostics, and food safety.

32 ***Keywords:***

33 *Aptasensor*

34 *Biosensor*

35 *Graphene*

36 *Aptamer*

37 *Two-dimensional nanomaterial*

38

39	<b>Content</b>
40	1. Introduction
41	2. Surface functionalization strategies for two-dimensional nanomaterials-based aptasensors
42	2.1. Non-covalent functionalization strategies
43	2.2. Covalent functionalization strategies
44	2.3. Decoration with metal nanoparticles for immobilization
45	3. Transduction methods for two-dimensional nanomaterials-based aptasensors
46	3.1. Electrochemical aptasensors
47	3.1.1. As transducers in electrochemical aptasensors
48	3.1.2. As nanocarriers in electrochemical aptasensors
49	3.1.3. Other electrochemical aptasensors
50	3.2. Optical aptasensors
51	3.2.1. Fluorescent aptasensors
52	3.2.2. Chemiluminescent aptasensors
53	3.3. Other transduction techniques for two-dimensional nanomaterials-based aptasensors
54	4. Conclusions
55	Acknowledgements
56	References
57	

## 58 **1. Introduction**

59 Nanomaterials have been employed to construct sensing devices in view of their  
60 unique electronic, optical, mechanical, and thermal properties. With the past decades,  
61 a new wave of research on the biosensors has focused on the combination of  
62 nanomaterials with molecular recognition elements (Wang et al., 2010a; Yang et al.,  
63 2010). Among the plethora of nanomaterials, two-dimensional nanomaterials have  
64 emerged as promising nanoplatforms. These next generation nanostructures have  
65 inherent superior light absorbance and rapid electron transfer rate (Georgakilas et al.,  
66 2012; Koski and Cui, 2013). Specifically, the unique planar structure and sizable  
67 specific surface areas would enlarge the loading efficiency and surface concentration  
68 of biomolecule (Chen et al., 2012b; Mao et al., 2013). Therefore, the integration of  
69 two-dimensional nanomaterials with aptamers could bring about many attractive  
70 opportunities for the development of novel aptasensors with enhanced performance.  
71 Here, we review the current research literature on two-dimensional  
72 nanomaterials-based aptasensors. Different aptasensing strategies along with different  
73 signal-transducing mechanisms and different combination modes of aptamers with  
74 two-dimensional nanomaterials are discussed. Our aim is to give the reader a  
75 complete concept about the recent advances of two-dimensional nanomaterials-based  
76 aptasensors and expect more two-dimensional nanostructures and more synthetic  
77 aptamers be enrolled into this research field that create really workable biosensing  
78 devices serving for human world.

79 Aptamers, generated from “systematic evolution of ligands by exponential  
80 enrichment” (SELEX) technique, are short single-stranded oligonucleotides (DNA or  
81 RNA) that bind to specific targets similarly as antibodies, drawing extensive attention  
82 from both the theoretical and experimental scientific communities since their  
83 discovery in 1990 (Ellington and Szostak, 1990; Robertson and Joyce, 1990; Tuerk  
84 and Gold, 1990). Aptamers act as molecular recognition elements whose purpose is to  
85 recognize and bind to their targets with excellent affinity (the dissociation constants

86  $K_d$  ranging from micromolar to picomolar levels) by folding themselves into distinct  
87 secondary or tertiary structures (Lubin and Plaxco, 2010; Wang et al., 2012f). The  
88 targets range from small organic molecules, metal ions, proteins, biological cells, to  
89 tissues (Amaya-Gonzalez et al., 2013). In addition, aptamers also exhibit other unique  
90 features over antibodies, such as *in vitro* selection, chemical stability, low  
91 immunogenicity, automated synthesis and numerous choices of nucleotide or  
92 phosphate functional groups (Du et al., 2013b). These exceptional properties make  
93 aptamers capable of serving as favorable molecular recognition elements in the design  
94 of high-performance biosensing devices (i.e., aptasensors) (Li et al., 2010;  
95 Vinkenborg et al., 2011) and reviews dealing with their biosensing strategies were  
96 published recently (Famulok and Mayer, 2011; Hong et al., 2012; Lim et al., 2010;  
97 Liu et al., 2009; Meir et al., 2007; Zhou et al., 2010).

98 Since the discovery of graphene, the field of two-dimensional nanomaterials has  
99 grown extensively over the past decade. So far, the family of two-dimensional  
100 nanomaterials has extended from graphene and its derivatives (like graphene oxide,  
101 fluorographene, graphane, etc.) to transition metal chalcogenides (such as  $\text{MoS}_2$ ,  $\text{WS}_2$ ,  
102  $\text{MoSe}_2$ ,  $\text{WSe}_2$ , etc.), metal oxides (like  $\text{MoO}_3$ ,  $\text{WO}_3$ ,  $\text{MnO}_2$ ,  $\text{Ni(OH)}_2$ , etc.), and other  
103 layered compounds with the common feature that the bulk three-dimensional crystals  
104 of these layered materials are stacked structures held together through their van der  
105 Waals forces among adjacent layers (Leonard and Talin, 2011; Xu et al., 2013a). A  
106 library of current two-dimensional crystals was made by Geim and Grigorieva (2013).  
107 By consecutive thinning of the bulk layered structures to monolayer or few-layer  
108 dimensions (i.e. two-dimensional), many intriguing properties are observed, such as  
109 topological insulator effect, superconductivity, and thermoelectricity (Govindaraju  
110 and Avinash, 2012; Koski and Cui, 2013).

111 Among these reported two-dimensional crystals, graphene deserves special  
112 recognition in view of its distinctive structure and exceptional physical properties  
113 (Novoselov et al., 2004). Graphene is a sheet of  $\text{sp}^2$  bonded carbon atoms that are

114 arranged into a rigid honeycomb lattice, exhibiting the highest mechanical strength  
115 among the known materials, extraordinary electron transfer capabilities, excellent  
116 electrical conductivity, ultra-large specific surface area, unprecedented pliability and  
117 impermeability, and favorable biocompatibility (Balandin, 2011; Craciun et al., 2011).  
118 Additionally, the methods of graphene synthesis have undergone substantial  
119 development in the past decade to meet various application requirements. Some  
120 examples of synthetic methods include mechanical exfoliation, chemical vapor  
121 method, chemical and electrochemical reduction methods to obtain either pristine  
122 graphene, single-layer graphene with designed plane size, or graphene composites  
123 directly from graphite, respectively (Park and Ruoff, 2009; Zhang et al., 2012a). All  
124 these promote the application prospects of graphene in electronic devices, energy  
125 generation and storage, sensors, DNA sequencing, and hybrid materials (Mao et al.,  
126 2013; Wu et al., 2007).

127 Regarding the aptasensor development, graphene looks like to have the  
128 necessary requirements to implement next generation, and high-performance  
129 aptasensors (Kuila et al., 2011). More importantly, graphene has a natural gift to  
130 noncovalent adsorption of the unfolded aptamer (i.e. aptamer chain in a flexible form)  
131 (through the  $\pi$ - $\pi$  stacking interaction between the puric and pyimidic bases of nucleic  
132 acid aptamers and the graphene plane) while repelling the adsorption of the folded  
133 aptamer (i.e. aptamer in a rigid three-dimensional structure) (Liu et al., 2012b; Park et  
134 al., 2014). The marriage of graphene and aptamers enables people to create many  
135 ingenious strategies for aptasensing applications. A variety of proof-of-concept  
136 aptasensors based on graphene have been designed (Fig. 1). Aptasensors based on  
137 other two-dimensional nanomaterials, such as transition metal chalcogenides and  
138 metal oxides, are also included below.

139 **Fig. 1**

## 140 **2. Surface functionalization strategies for two-dimensional nanomaterials-based** 141 **aptasensors**

142 One of the key considerations for the fabrication of an aptasensor is the  
143 immobilization of aptamers onto the surface of transducer, as the basis of the  
144 detection of the target molecule relies on its interaction with the former. For the inert  
145 graphitic structure, a pre-functionalization step is necessary prior to biomolecule  
146 immobilization. The currently developed strategies for graphene functionalization  
147 include covalent and non-covalent approaches. Conventional covalent treatments  
148 often include an oxidative functionalization that may damage graphene properties.  
149 Non-covalent approach relies mainly on  $\pi$ - $\pi$  stacking interactions.

### 150 *2.1. Non-covalent functionalization strategies*

151 The non-covalent approach enables modifying graphene with desired functional  
152 groups, without affecting its intrinsic properties. Physical adsorption is the simplest  
153 immobilization method in the graphene-based aptasensors in view of the favorable  
154 feature of  $\pi$ - $\pi$  stacking interaction between the puric and pyrimidic bases of aptamers  
155 and the hexagonal cells of graphene (Park et al., 2012). Du et al. used a graphene  
156 modified electrode to bind aptamer by physical adsorption (Du et al., 2012a). The  
157 recognition of the target protein in the solution led to a neutralization of the negatively  
158 charged phosphate backbone of the aptamer, resulting in the decrease of the  
159 electrochemical signals of cationic ruthenium complex. Another procedure for  
160 non-covalent functionalization relies on the use of polyaromatic hydrocarbons that  
161 strongly adsorb on graphene through  $\pi$ - $\pi$  stacking interaction (Sun et al., 2013). The  
162 use of pyrene butyric acid for example, enables a stable and robust functionalization  
163 through  $\pi$ - $\pi$  stacking of the four aromatic rings, while the terminal acid function  
164 remains free and available for further covalent grafting of biomolecules through their  
165 amine functions (Kong et al., 2013). This procedure offers the advantages of the  
166 covalent grafting without altering the graphitic properties.

167 Besides physical adsorption approach, electrostatic adsorption is another method  
168 in the assembly of aptamers onto transducers. The negatively charged aptamers can be  
169 electrostatically adsorbed onto positively charged transducers in neutral buffers of low

170 osmolarity (< 100 mM). By functionalization of graphene with charged materials, like  
171 poly(sodium 4-styrenesulfonate) (Qin et al., 2012) and Fe<sub>2</sub>O<sub>3</sub> (Du et al., 2013a), simple  
172 and label-free electrochemical aptasensors were constructed.

### 173 ***2.2. Covalent functionalization strategies***

174 The covalent approach often relies on the oxidation of graphene. Indeed,  
175 graphene samples prepared by the oxidative methods or by the reduction of graphene  
176 oxide initially carry carbonyl and carboxyl functional groups (Biju, 2014). These  
177 groups can be coupled with biomolecules through their amine functions. Chemical  
178 oxidation of graphene enables increasing the density of carbonyl and carboxyl  
179 functional groups and is widely used for the chemical modification of the inert  
180 graphitic structure (Maiti et al., 2014). However, this procedure strongly affects the  
181 properties of graphene. The covalent modification of graphitic surface is also possible  
182 without a pre-oxidation step, through a free radical addition reaction, expected to have  
183 less impact on the electronic properties (Bekyarova et al., 2009). Besides the  
184 immobilization methods above, amide (Xiao et al., 2013) and phosphoramidate  
185 reactions (Liu et al., 2012a) were employed towards the fabrication of graphene-based  
186 aptasensors. In addition, some graphene derivatives, such as GO, were used as  
187 transducers in electrochemical aptasensors (Yan et al., 2013b).

### 188 ***2.3. Decoration with metal nanoparticles for immobilization***

189 Graphene can be decorated with metal nanoparticles to enhance the signal of the  
190 transduction techniques or to increase the grafting area for aptamer immobilization  
191 (Rao et al., 2009). Gold nanoparticles (AuNPs) are the mostly founded metal  
192 nanoparticles in graphene-aptamer based biosensing system, since gold could form  
193 strong covalent bond (Au-S) with thiol group. An electrochemical aptasensor using  
194 graphene-AuNPs composite obtained by the reduction of tetrachloroauric acid with  
195 sodium citrate in a graphene water suspension was reported (Liang et al., 2011). In  
196 order to simplify the fabrication method, direct electrodeposition technique of AuNPs  
197 was also applied to electrochemical aptasensors. This method could produce graphene

198 transducers with a high-density of AuNPs that provide ultra-large specific surface area  
199 for aptamer immobilization (Jiang et al., 2012a). Most of graphene-based  
200 electrochemical aptasensors are constructed in this way, including probe-free and  
201 sandwich types. Recently, a simpler method to form graphene-AuNPs transducer by  
202 simultaneous electrodeposition of graphene and AuNPs onto the electrode surface was  
203 developed (Zheng et al., 2013). Two leukemia-type aptamers (sgc8c and KH1C12)  
204 were assembled on this transducer to capture the target cells and another layer of  
205 aptamers labeled with different redox tags were formed on the cell surface (Fig. 2a).  
206 By this strategy, they demonstrated an effective method for simultaneous detection of  
207 multiple leukemia-type cells.

208 **Fig. 2**

### 209 **3. Transduction methods for two-dimensional nanomaterials-based aptasensors**

#### 210 **3.1. Electrochemical aptasensors**

211 Electrochemical methods have been extensively recognized as a powerful tool  
212 for fast access to (bio)chemical information in complex samples in view of their high  
213 sensitivity, fast response, easy operation, and low-cost. In a typical electrochemical  
214 aptasensing system, nucleic acid aptamers are immobilized on a conducting substrate  
215 (i.e., transducer). When binding to their target molecules, they fold their flexible  
216 chains into well-defined three-dimensional structures (Song et al., 2008). This  
217 behavior enables redox-active species-labeled aptamers to have a dynamic distance to  
218 the transducer (label type) or in solution to have a different steric hindrance in getting  
219 closer to the transducer (label-free type). Consequently, the formation of the  
220 aptamer-target complexes could be identified by probing the electron-transfer kinetics  
221 of the redox species.

##### 222 **3.1.1. As transducers in electrochemical aptasensors**

223 Graphene-based electrochemical transducers have shown many excellent  
224 properties, such as wide electrochemical window, high signal/noise ratio, fast electron  
225 transfer kinetics, and more importantly the feasibility for composite incorporation,

226 which make them attractive platforms in electrochemical aptasensors (Chen et al.,  
227 2010; Huang et al., 2012; Ping et al., 2011). Table 1 summarizes the recent progress of  
228 graphene-based transducers for electrochemical aptasensors.

229 **Table 1**

230 Zhao et al. reported a graphene quantum dots (QDs)-based electrochemical  
231 aptasensor for the detection of thrombin, in which the aptamers were physically  
232 adsorbed onto graphene QDs surface and the redox specie  $[\text{Fe}(\text{CN})_6]^{3-/4-}$  was used as  
233 electrochemical probe (Zhao et al., 2011). By incorporation of redox-active species  
234 into the graphene-based transducer, probe-free detection was achieved. Additionally, a  
235 high-throughput and reusable aptasensing platform was established (Tang et al., 2011a)  
236 with magnetic graphene nanosheets as transducer. They further improved the  
237 detection system by coupling nuclease cleavage (DNase I) for signal amplification  
238 and distinguishable redox tag-conjugated aptamers for multiplex analysis (Fig. 2b)  
239 (Tang et al., 2011b).

240 Recently, the performance of various graphene materials, such as GO,  
241 electrochemically reduced graphene, and thermally reduced graphene was compared  
242 (Loo et al., 2012). Results showed that GO was the most sensitive platform for  
243 thrombin aptasensing. Furthermore, the different immobilization methods on the  
244 effect of impedance response of GO-based aptasensors were also studied (Loo et al.,  
245 2013a). It was discovered that while all three immobilization methods uniformly show  
246 a similar optimum amount of immobilized aptamer, physical and covalent  
247 immobilization methods exhibit higher selectivity than affinity immobilization.

248 **3.1.2. As nanocarriers in electrochemical aptasensors**

249 Another interesting application of graphene and its derivative in electrochemical  
250 aptasensors is to be used as a nanocarrier to load electroactive species, enzymes or  
251 recognition molecules (Table 2). As mentioned previously, graphene nanosheets have  
252 unusually large surface areas with the ability to incorporate various inorganic or  
253 organic species to build a multifunctional nanocarrier (Huang et al., 2012). That is,

254 graphene nanosheets could covalently attach or physically adsorb signal molecules  
255 and/or recognition elements on their surface. When using this nanocarrier to construct  
256 electrochemical aptasensors, it can significantly enlarge the loading of signal  
257 molecules and consequently increase the sensitivity. An electrochemical sandwich  
258 aptasensor for simultaneous detection of platelet-derived growth factor and thrombin  
259 was fabricated (Fig. 3a) (Bai et al., 2012b). Two graphene-based nanocarriers with  
260 different redox probes were synthesized and further used as the labels for aptamers  
261 through a sandwich assay in order to amplify the signals. Such an approach has  
262 demonstrated the capability of graphene-based nanocarriers to achieve a substantial  
263 amplification. GO was also used as nanocarrier in electrochemical aptasensors (Wang  
264 et al., 2012d). Chen et al. reported two simple probe-label-free electrochemical  
265 aptasensing strategies based on GO constructed nanocarriers (Chen et al., 2013).

266

## Table 2

267

## Fig. 3

### 268 *3.1.3. Other electrochemical aptasensors*

269 In addition to acting as transducers and nanocarriers in electrochemical  
270 aptasensors, graphene can also mediate electron-transfer in view of the high-density  
271 edge-plane-like defects present within its nanostructure (Ping et al., 2012). A  
272 label-free electrochemical aptasensor was constructed by taking advantage of the  
273 ultra-fast electron transfer ratio of graphene (Wang et al., 2012a). In the absence of  
274 target, aptamers immobilized on the gold electrode would adsorb graphene nanosheets  
275 due to the strong  $\pi$ - $\pi$  interaction that accelerate the electron transfer ratio between the  
276 electroactive species and the electrode surface. In the presence of target, the binding  
277 reaction would inhibit the adsorption of graphene and block electron transfer. Yan et  
278 al. further improved this detection strategy by nuclease cleavage-assisted target  
279 recycling amplification yielding a detection limit of 0.065 pM for interferon-gamma  
280 (Yan et al., 2013a). Pumera's group employed graphene oxide nanoplatelets (GONPs)

281 as inherently electroactive labels for thrombin detection (Loo et al., 2013b). Their  
282 design consisted of GONPs with a dimension of  $50 \times 50$  nm which has a reduction  
283 peak near  $\sim 1.2$  V that can be used as an analytical signal. The different affinity of  
284 GONPs to unbound aptamers versus target-bound aptamers enabled GONPs to be  
285 utilized as an effective label for sensitive detection of thrombin (Fig. 3b).

### 286 ***3.2. Optical aptasensors***

287 Optical aptasensing assays have been extensively used in medical diagnosis and  
288 environmental monitoring, due to their high sensitivity and simple readout devices  
289 (Chen et al., 2011; Wang et al., 2010a). The introduction of two-dimensional  
290 nanomaterials into optical aptasensors could eliminate the separation step and  
291 improve analytical performance since the two-dimensional nanostructures possess  
292 unique plane structure and optical properties (Du et al., 2013b). Recent studies on  
293 two-dimensional nanostructures-based optical aptasensors mainly focus on  
294 fluorescence and chemluminescence. Although GO is the most widely studied  
295 nanomaterial in optical aptasensing assays, other two-dimensional nanomaterials are  
296 also attracting attention, such as single-layer molybdenum sulfide ( $\text{MoS}_2$ ) and carbon  
297 nitride nanosheet (CNNS).

#### 298 ***3.2.1. Fluorescent aptasensors***

299 Fluorescence is a commonly used signal transducing mechanism in  
300 aptamer-based assays in view of its sensitivity, and convenience. Since the aptamers  
301 can be easily labeled with various fluorophores (such as organic dyes and  
302 nanomaterials), approaches have focused on how to detect the changes of  
303 fluorescence intensity in response to target-aptamer binding (Wang et al., 2011b).  
304 Until now, there are two commonly used detection modes in fluorescent aptasensors,  
305 i.e. detection based on the change of fluorescent intensity (quenching or restoring of  
306 fluorescent molecules) and detection based on the change of fluorescent anisotropy  
307 (aka fluorescent polarization).

#### 308 ***Sensing by change in fluorescent intensity***

309 Fluorescence resonance energy transfer (FRET) is a nonradiative process in  
310 which a donor within excited state transfers energy to a proximal acceptor within a  
311 ground state and is commonly found in optical aptasensors (Zhang et al., 2013b). In a  
312 well-designed FRET-based aptasensing mode, the fluorophore (i.e. electron donor)  
313 and quencher (i.e. electron acceptor) are brought into proper distance from each other  
314 exclusively via the binding process. The low FRET efficiency and  $R^{-6}$  response  
315 dependence of the FRET fluorophore-quencher molecules requires careful design to  
316 avoid large background signals (Citartan et al., 2012). Two-dimensional nanomaterials  
317 may overcome these design limitations in view of their excellent  
318 fluorescence-quenching capability by intrasheet energy or electron-transfer. GO is  
319 commonly employed in FRET-based aptasensor designs with many advantages (Chen  
320 et al., 2012b). GO's hydrophilic nature and water miscibility facilitates homogeneous  
321 fluorescent signals. As an electron acceptor, GO can be employed as a generic  
322 quencher for numerous fluorophores, including organic dyes, conjugated polymers,  
323 and quantum dots. The quenching by GO is through long range resonance energy  
324 transfer (LrRET) which has  $R^{-4}$  dependence from the fluorophore (Liu et al., 2013a).  
325 Much like graphene, GO varies its response in regards to unfolded versus folded  
326 aptamers (i.e. upon binding to a target, a change in the aptamer tertiary structure will  
327 allow changes in fluorescent intensity). Such a design allows multiplexed FRET  
328 analysis towards multiple labeled aptamers on single GO sheet. Furthermore, with  
329 GO's inherent steric-hindrance, biomolecules may be protected from enzymatic  
330 degradation. Various GO-based FRET aptasensing assays are listed in Table 3.

331

### Table 3

332 In a typical GO-based FRET aptasensing mode, aptamer firstly adsorbs onto the  
333 surface of GO and the labeled fluorophore is quenched by the GO (Fig. 4a). The  
334 binding reaction induces a conformational change of aptamer that enables the  
335 aptamer-target conjugate to dissociate from the GO and consequently the fluorescence  
336 of fluorophore is restored (Chang et al., 2010). Various fluorescent species, including

337 organic dyes and quantum dots, have been used in this sensing mode to detect small  
338 molecules and proteins (Dong et al., 2010). Huang et al. have carefully studied the  
339 effect of solution pH on the adsorption of aptamer to GO and the binding of aptamer  
340 to its target (Huang et al., 2011). They found these two processes could be controlled  
341 by tuning the solution pH. That means GO/aptamer based FRET sensing system could  
342 be easily restored.

#### 343 **Fig. 4**

344 In order to improve sensitivity, several amplification strategies were explored.  
345 One effective method is to incorporate the nucleic acid-related enzymes into the  
346 detection process. As mentioned above, GO can protect the adsorbed aptamer from  
347 the enzymatic digestion. Inspired by this, deoxyribonuclease I (DNase I) was used to  
348 cleave the unadsorbed aptamer (Fig. 4b) (Lu et al., 2010). A much lower detection  
349 limit (40 nM) was achieved for the ATP detection which was ~250-fold lower than  
350 that of the strategy without DNase I (10  $\mu$ M). Exonuclease III (Exo III), a  
351 double-stranded specific enzyme, was also used to amplify the fluorescent signal in  
352 GO-based FRET sensing (Chen et al., 2012a). Besides these nucleic acid lyases, Hu et  
353 al. employed polymerase Klenow fragment induced strand-displacement  
354 polymerization reaction to realize the highly sensitive detection of interferon-gamma  
355 (Fig. 4c) at a quite low detection limit of 1.5 fM (Hu et al., 2013).

356 Another approach for sensitivity enhancement is to tuning the distance between  
357 the fluorophore and GO. GO is an excellent quencher with an effective quenching  
358 distance of  $R^{-4}$  dependence that enables LrRET in the sensing process (Zhuang et al.,  
359 2013). Ueno et al. used a DNA spacer modified on aptamer to control the distance  
360 between the fluorophore and GO (Ueno et al., 2013). By carefully screening the  
361 length of spacer, a detection limit of ~1 nM for thrombin was obtained. Zhuang et al.  
362 employed LrRET as the signal transducing mechanism to detect cellular prion protein  
363 with a detection limit of 0.309  $\mu$ g mL<sup>-1</sup> (Zhuang et al., 2013).

364 An important issue in GO-based aptasensing is the multiplexed detection.

365 GO-based aptamer logic gates for simultaneous detection of ATP and thrombin was  
366 developed (Wang et al., 2012b). A paper-based microfluidic biochip integrated with  
367 GO and aptamer for fluorescent detection of two infectious pathogens was also  
368 developed (Zuo et al., 2013). Recently, a highly tunable GO microarray has been  
369 devised for high-throughput multiplexed protein sensing (Fig. 5) (Jung et al., 2013). A  
370 thin GO film building from layer-by-layer assemble technique was used as an  
371 excellent quencher of dye-labeled aptamers. By optimizing the layers of the GO film  
372 and constructing a microarray, four different targets could be detected simultaneously.

373

### Fig. 5

374 Besides being a quencher, GO could be used as a fluorescent specie (i.e. electron  
375 donor) in FRET-based aptasensors. Shi et al. fabricated a fluorescent aptasensor based  
376 on a structure switchable aptamer, GNPs, and GO for the detection of cocaine (Shi et  
377 al., 2013). In the presence of cocaine, its corresponding aptamer folds into a  
378 three-way junction that shortens the distance of donor (GO) and acceptor (GNPs)  
379 resulting in the decrease of fluorescent intensity of the GO. In another work, a  
380 thymine-rich aptamer with a GO-based fluorophore was used to detect  $\text{Hg}^{2+}$  (Li et al.,  
381 2013a). The thymine-rich aptamer can bind with  $\text{Hg}^{2+}$  due to the formation of the  
382 thymine- $\text{Hg}^{2+}$ -thymine complex, which brings the  $\text{Hg}^{2+}$  near the GO surface. If these  
383 mercury ions are close enough, they quench the fluorescence of GO through electron  
384 transfer from GO along the duplex DNA channel.

385 Other two-dimensional nanomaterials were also employed into FRET-based  
386 aptasensors. Single-layer  $\text{MoS}_2$  possesses high fluorescence-quenching capability and  
387 exhibits different interaction toward unfolded and folded ssDNA (Zhu et al., 2013a).  
388 Fluorophore labeled aptamer was mixed with target and then  $\text{MoS}_2$  was subsequently  
389 added. The poor affinity between  $\text{MoS}_2$  nanosheets and aptamer-target conjugates  
390 resulted in no loss of fluorescence and a quantitative readout for the target (adenosine)  
391 was possible with a detection limit of 5  $\mu\text{M}$ . Ge et al. extended this  
392 nanomaterials-based FRET to thrombin target (Fig. 6a) (Ge et al., 2014). Manganese

393 dioxide ( $\text{MnO}_2$ ) nanosheets could also be used as an effective energy acceptor. Yuan  
394 et al. fabricated two aptasensors for the homogeneous analysis of ochratoxin A and  
395 cathepsin D based on the  $\text{MnO}_2$  nanosheets acting as nanoquencher and upconversion  
396 phosphors labeled aptamers acting as bioprobes (Fig. 6b) (Yuan et al., 2014).

397 **Fig. 6**

398 In addition to the FRET-based detection mode, other signal transducing  
399 mechanisms were also introduced into the sensing by the change of fluorescence  
400 intensity. Wu's group reported a 'turn-on' fluorescent aptasensor through nano-metal  
401 surface energy transfer (NSET) from CdSe/ZnS QDs to GO (Li et al., 2013b). NSET  
402 typically possesses a longer energy transfer distance than FRET and does not need a  
403 resonant interaction between the electrons but rather an interband electronic transition.  
404 Based on this fluorescent quenching mechanism, a lower detection limit of 90 pM was  
405 obtained for  $\text{Pb}^{2+}$  detection. Another fluorescent quenching mechanism is based on the  
406 photoinduced electron transfer (PET) process. Recently, Wang et al. developed a  
407 carbon nitrite nanosheet (CNNS)-based fluorescent aptasensor for  $\text{Hg}^{2+}$  detection  
408 (Wang et al., 2013a). They found the fluorescence quenching followed a static  
409 quenching through the PET from the excited fluorophore to the conductive band of  
410 CNNS. As a result, a detection limit of 16 nM for  $\text{Hg}^{2+}$  detection was achieved.

#### 411 *Sensing by change in fluorescent anisotropy*

412 Fluorescence anisotropy (FA) is another fluorescent signal transducing method  
413 that provides information about the molecular mobility, orientation, and interaction  
414 process through changes in the molecular weight of the fluorescent species (Liu et al.,  
415 2013c). It is a well-documented method to detect biologically related macromolecules  
416 by coupling with dye-labeled aptamers (Gokulrangan et al., 2005). However, it is hard  
417 to detect small molecule targets as changes in low molecular mass cannot produce  
418 appropriate changes in observable anisotropy (Zhang et al., 2011a). To address this  
419 issue, Liu et al. developed an aptasensing strategy based on FA signal amplification  
420 by using GO as the signal amplifier (Liu et al., 2013b). Fig. 7 shows two strategies of

421 GO-based FA detection. For the FA reduction assay ('signal off' mode), a fluorescein  
422 labeled aptamer adsorbs on the surface of GO, where its rotation is constrained  
423 resulting in a high fluorescence anisotropy. In the presence of target, the structure  
424 change of aptamer induces desorption of aptamer from GO and a subsequent decrease  
425 of FA. While in the 'signal on' mode (FA enhancement assay), a fluorescent  
426 dye-labeled complementary ssDNA to aptamer (that could form a dsDNA with low  
427 anisotropy signal) is used as a signaling probe. When displaced by the target, the  
428 released ssDNA is adsorbed onto the surface of GO inducing an increase in the  
429 anisotropy value. By this approach, they demonstrated a sensitive aptasensor for ATP  
430 detection. A similar FA transducing strategy for copper ion detection was also  
431 developed (Yu et al., 2013a).

### 432 **Fig. 7**

#### 433 **3.2.2. Chemiluminescent aptasensors**

434 Chemiluminescent (CL) detection has been widely used in various fields, due to  
435 its sensitive, simple, and inexpensive characteristics (Cho et al., 2014). Compared to  
436 the fluorescence, it does not require an external light source, and the life time of the  
437 luminescence species is much longer than that of fluorescent ones. Taking advantage  
438 of this method, a CL detection system was established on the basis of the excellent  
439 luminescence quenching capability of GO through chemiluminescent resonance  
440 energy transfer (CRET) and the interaction of unfolded aptamer with GO (Choi and  
441 Lee, 2013). Furthermore, by introduction of magnetic beads ( $\text{Fe}_3\text{O}_4$ ) on GO  
442 nanosheets, the impurities in human serum samples capable of reducing the efficiency  
443 of the aptasensor were removed and rapid detection of prostate specific protein was  
444 realized. A label-free CL aptasensor for ATP detection was developed (Song et al.,  
445 2014), in which a CL reagent phenylglyoxal was used as the signal reporter that could  
446 react specifically with guanine bases of aptamer adsorbed on the GO surface. The  
447 presence of ATP would release the aptamer from GO nanosheets that induce the  
448 decrease of the CL signal.

449 Electrogenerated chemiluminescence (ECL) is another effective detection  
450 method in aptasensing due to the combination of the electrochemical advantages with  
451 CL sensitivity (Wang et al., 2013b; Zhou et al., 2013). Like graphene-based  
452 electrochemical aptasensors, graphene also could be used as transducer and  
453 nanocarrier in ECL aptasensors with enhanced performance (Gan et al., 2012; Liao et  
454 al., 2011; Xie et al., 2013; Yu et al., 2013b). Recently, Wei et al. developed a sensitive  
455 aptasensor for the detection of mucin 1 protein and MCF-7 cells based on ECL  
456 resonance energy transfer from a ruthenium complex to GO (Wei et al., 2012). Jin et  
457 al. reported a GO-based ECL detection approach using an iridium complex as the  
458 ECL reagent (Jin et al., 2013). An interesting ECL system using graphene QDs was  
459 explored to detect ATP (Lu et al., 2013). Graphene QDs exhibit bright blue emission  
460 under ultraviolet irradiation and could combine with H<sub>2</sub>O<sub>2</sub> as a coreactant in ECL  
461 detection. By employing SiO<sub>2</sub> nanospheres as a signal carrier, a sensitive aptasensor  
462 for the detection of ATP was constructed through a SiO<sub>2</sub>/Graphene QDs-based ECL  
463 signal amplification strategy.

### 464 *3.3 Other transduction techniques for two-dimensional nanomaterials-based* 465 *aptasensors*

466 Besides the electrochemical and optical transducing mechanisms mentioned  
467 previously, a number of other transducing mechanisms have been proposed in  
468 two-dimensional nanomaterials-based aptasensors. Electronic detection based on  
469 field-effect transistor (FET) is an effective method (Willner and Zayats, 2007).  
470 Graphene-based FET has shown great potential for the sensitive determination of  
471 various analytes (He et al., 2012a; Liu et al., 2012b). In a typical graphene-based FET  
472 sensing system, graphene sheets were coated on a Si/SiO<sub>2</sub> substrate to obtain a  
473 channel (Ohno et al., 2010). Then a small organic molecule (1-pyrenebutanoic acid  
474 succinimidyl ester) was used as a linker to attach the aptamer onto the graphene sheet.  
475 The binding reaction between aptamer and target can induce an effect on the  
476 charge-carrier density on the surface of the graphene plane, and consequently it may

477 allow label-free detection of analytes. One key factor in the design of a FET  
478 aptasensor is to ensure the binding reaction of aptamer-ligand occurs within the  
479 Debye length since the charge change in the area outside the Debye length cannot  
480 induce the carriers change of graphene (Ohno et al., 2010). Graphene nanosheets  
481 made from mechanical exfoliation and chemical reduction have been used to fabricate  
482 FETs for aptasensing IgE, thrombin, and cocaine (Ohno et al., 2010 and 2011). A FET  
483 based on polypyrrole-converted nitrogen-doped few-layer graphene was developed  
484 (Kwon et al., 2012). By doping the graphene planar lattice with nitrogen atoms, the  
485 band gap of graphene was opened and consequently a stable *n*-type  
486 (electron-transporting) behavior was observed (Fig. 8a). A sandwich-type  
487 graphene-based FET was reported (Kim et al., 2013), in which secondary  
488 aptamer-conjugated gold nanoparticles was used to increase the charge-doping in  
489 graphene channel (Fig. 8b) and a ultra-low detection limit of 1.2 aM for a protective  
490 antigen was obtained in that detection mode. A graphene-based FET aptasensor based  
491 on aptazyme modified AuNPs for the detection of Pb<sup>2+</sup> with a detection limit at the  
492 nM level was developed (Wen et al., 2013). Surface plasmon resonance (SPR) is  
493 another transducing mechanism in graphene-based aptasensors (Subramanian et al.,  
494 2013). A SPR aptasensing platform based on graphene film for thrombin detection  
495 was recently reported (Wang et al., 2011a). Prior to the detection, graphene sheets  
496 were assembled on a positively charged SPR gold film via electrostatic interaction  
497 and the target aptamer was noncovalently adsorbed onto the graphene sheets (Fig. 8c).  
498 The binding reaction between the aptamer and target would greatly disturb the  
499 interaction between the aptamer and graphene that took off the aptamer from the  
500 graphene surface resulting in a decreased SPR angle. Finally, Zhang et al. recently  
501 developed a quartz crystal microbalance aptasensor for thrombin detection based on  
502 an amino-functionalized nanocomposite of graphene and plasma-polymerized  
503 allylamine (Zhang et al., 2014). They found that the presence of graphene enhances  
504 the electrochemical activity of the plasma and improves the sensitivity of the resulting

505 aptasensor, opening a promising use of these materials in piezoelectric transduction.

506 **Fig. 8**

#### 507 **4. Conclusions**

508 This work has presented an overview about current advances in the development  
509 and application of two-dimensional nanomaterials-based aptasensors. Different types  
510 of two-dimensional nanomaterials have been employed to explore aptasensors with a  
511 range of signal transducing mechanisms, such as electrochemical, optical, and so on.  
512 Significantly, some reagent-free and one-step analysis strategies have been established  
513 by the assembly of two-dimensional nanostructures with aptamers. However, despite  
514 these advances, graphene and graphene-like two-dimensional nanomaterials-based  
515 aptasensors are still relatively immature in development compared to other biosensing  
516 tools. Many technical hurdles still need to be addressed, including the desorption of  
517 bioelements and nanomaterials from the aptasensing devices over time, the effect of  
518 non-uniform two-dimensional nanomaterials (i.e. due to shifts in nanomaterial size or  
519 shape) on performance of aptasensing devices, and the low affinity and specificity of  
520 aptamers towards inorganic small molecules.

521 Additionally, some important issues and challenges should be prioritized.  
522 Current studies are mainly on graphene and its derivative-based aptasensors. Recently,  
523 other two-dimensional nanomaterials with unique features have been synthesized. For  
524 example, recent studies have shown that single-layer MoS<sub>2</sub> constructed FET displays  
525 a room-temperature On/Off ratio exceeding 10<sup>8</sup> (Wang et al., 2012c). That would help  
526 MoS<sub>2</sub> two-dimensional nanomaterials in the construction of high-performance FET  
527 aptasensors (Huang et al., 2013). On the other hand, the analytes of aptasensors  
528 should be diversified, not limited to thrombin and ATP even they are important in  
529 biology. Almost all of the current two-dimensional nanomaterials-based aptasensors  
530 use DNA aptamers as the molecular recognition element. The reports on combination  
531 of RNA aptamers with two-dimensional nanomaterials constructed aptasensors are  
532 rarely found, probably due to their expensive synthesis and inherent instability.

533 Nevertheless, RNA aptamers have higher affinity towards their targets than DNA  
534 aptamers. They also show more abundant structural information changes upon  
535 binding that enables more sensitive and simpler aptasensing strategies (Patel et al.,  
536 1997).

537 An important challenge of two-dimensional nanomaterials-based aptasensors is  
538 the practical application, i.e. analysis of analytes in real world, complex environments.  
539 Two main issues should be considered in this context. One is the sample matrix effect,  
540 since the real sample (e.g. body fluids, wastewater) always contain a mixture of  
541 macromolecules, ions, and particles that would induce a nonspecific signal in the  
542 detection process. Therefore, research work focusing on aptasensors should explore  
543 the feasibility of aptasensors and their recognition limits in complex environments.  
544 Typically, most reported results were performed in optimal laboratory conditions. The  
545 last issue is scalable methods of fabrication. Most fabrication techniques for  
546 aptasensors are designed for fast production at laboratory scales and are unable to be  
547 scaled for rapid production. If aptasensors are to be routinely commercialized,  
548 ubiquitous, scalable methods of synthesis need to be developed to produce greater  
549 amounts of aptasensors that are ISO compliant, have reproducible specifications, and  
550 can be made from cheap starting materials. Such a technique is the prerequisite for the  
551 successful commercial application of any aptasensing devices. Nevertheless, we  
552 expect that these two-dimensional nanomaterials-based aptasensing devices will  
553 eventually become an effectively routine analysis tool that could meet various  
554 challenges.

## 555 **Acknowledgements**

556 This Research is conducted by NTU-HUJ-BGU Nanomaterials for Energy and Water  
557 Management Programme under the Campus for Research Excellence and  
558 Technological Enterprise (CREATE), that is supported by the National Research  
559 Foundation, Prime Minister's Office, Singapore. Funding was also greatly appreciated  
560 from the Ministry of Education Tier 1 Grants: RG46/11, RG54/13, and Tier 2 grant:

561 MOE2012-T2-2-046.

562 **References**

- 563 Amaya-Gonzalez, S., de-los-Santos-Alvarez, N., Miranda-Ordieres, A.J., Lobo-Castanon, M.J., 2013.  
564 Sensors 13, 16292-16311.
- 565 Bai, L.J., Yan, B., Chai, Y.Q., Yuan, R., Yuan, Y.L., Xie, S.B., Jiang, L.P., He, Y., 2013. Analyst 138,  
566 6595-6599.
- 567 Bai, L.J., Yuan, R., Chai, Y.Q., Yuan, Y.L., Wang, Y., Xie, S.B., 2012a. Chem. Commun. 48,  
568 10972-10974.
- 569 Bai, L.J., Yuan, R., Chai, Y.Q., Zhuo, Y., Yuan, Y.L., Wang, Y., 2012b. Biomaterials 33, 1090-1096.
- 570 Balandin, A.A., 2011. Nat. Mater. 10, 569-581.
- 571 Bekyarova, E., Itkis, M.E., Ramesh, P., Berger, C., Sprinkle, M., de Heer, W.A., Haddon, R.C., 2009. J.  
572 Am. Chem. Soc. 131, 1336-1337.
- 573 Biju, V. 2014. Chem. Soc. Rev. 43, 744-764.
- 574 Chang, H.X., Tang, L.H., Wang, Y., Jiang, J.H., Li, J.H., 2010. Anal. Chem. 82, 2341-2346.
- 575 Chen, C.F., Zhao, J.J., Jiang, J.H., Yu, R.Q., 2012a. Talanta 101, 357-361.
- 576 Chen, D., Feng, H.B., Li, J.H., 2012b. Chem. Rev. 112, 6027-6053.
- 577 Chen, D., Tang, L.H., Li, J.H., 2010. Chem. Soc. Rev. 39, 3157-3180.
- 578 Chen, J.R., Jiao, X.X., Luo, H.Q., Li, N.B., 2013. J. Mater. Chem. B 1, 861-864.
- 579 Chen, T., Shukoor, M.I., Chen, Y., Yuan, Q.A., Zhu, Z., Zhao, Z.L., Gulbakan, B., Tan, W.H., 2011.  
580 Nanoscale 3, 546-556.
- 581 Cho, S., Park, L., Chong, R., Kim, Y.T., Lee, J.H., 2014. Biosens. Bioelectron. 52, 310-316.
- 582 Choi, H.K., Lee, J.H., 2013. Anal. Methods 5, 6964-6968.
- 583 Citartan, M., Gopinath, S.C.B., Tominaga, J., Tan, S.C., Tang, T.H., 2012. Biosens. Bioelectron. 34,  
584 1-11.
- 585 Craciun, M.F., Russo, S., Yamamoto, M., Tarucha, S., 2011. Nano Today 6, 42-60.
- 586 Deng, K., Xiang, Y., Zhang, L.Q., Chen, Q.H., Fu, W.L., 2013. Anal. Chim. Acta 759, 61-65.
- 587 Dong, H.F., Gao, W.C., Yan, F., Ji, H.X., Ju, H.X., 2010. Anal. Chem. 82, 5511-5517.
- 588 Du, M., Yang, T., Guo, X.H., Zhong, L., Jiao, K., 2013a. Talanta 105, 229-234.
- 589 Du, M., Yang, T., Zhao, C.Z., Jiao, K., 2012a. Sens. Actuators, B 169, 255-260.
- 590 Du, Y., Guo, S.J., Qin, H.X., Dong, S.J., Wang, E.K., 2012b. Chem. Commun. 48, 799-801.
- 591 Du, Y., Li, B.L., Wang, E.K., 2013b. Acc. Chem. Res. 46, 203-213.
- 592 Ellington, A.D., Szostak, J.W., 1990. Nature 346, 818-822.
- 593 Famulok, M., Mayer, G., 2011. Acc. Chem. Res. 44, 1349-1358.
- 594 Feng, L.Y., Chen, Y., Ren, J.S., Qu, X.G., 2011. Biomaterials 32, 2930-2937.
- 595 Gan, X.X., Yuan, R., Chai, Y.Q., Yuan, Y.L., Cao, Y.L., Liao, Y.H., Liu, H.J., 2012. Anal. Chim. Acta  
596 726, 67-72.

597 Ge, J., Ou, E.C., Yu, R.Q., Chu, X., 2014. *J. Mater. Chem. B* 2, 625-628.

598 Geim, A.K., Grigorieva, I.V., 2013. *Nature* 499, 419-425.

599 Georgakilas, V., Otyepka, M., Bourlinos, A.B., Chandra, V., Kim, N., Kemp, K.C., Hobza, P., Zboril, R.,  
600 Kim, K.S., 2012. *Chem. Rev.* 112, 6156-6214.

601 Gokulrangan, G., Unruh, J.R., Holub, D.F., Ingram, B., Johnson, C.K., Wilson, G.S., 2005. *Anal. Chem.*  
602 77, 1963-1970.

603 Govindaraju, T., Avinash, M.B., 2012. *Nanoscale* 4, 6102-6117.

604 Guo, Y.J., Han, Y.J., Guo, Y.X., Dong, C., 2013. *Biosens. Bioelectron.* 45, 95-101.

605 Han, J., Zhuo, Y., Chai, Y.Q., Yuan, R., Xiang, Y., Zhu, Q., Liao, N., 2013. *Biosens. Bioelectron.* 46,  
606 74-79.

607 He, Q.Y., Wu, S.X., Yin, Z.Y., Zhang, H., 2012a. *Chem. Sci.* 3, 1764-1772.

608 He, Y., Lin, Y., Tang, H.W., Pang, D.W., 2012b. *Nanoscale* 4, 2054-2059.

609 He, Y., Wang, Z.G., Tang, H.W., Pang, D.W., 2011. *Biosens. Bioelectron.* 29, 76-81.

610 Hong, P., Li, W.L., Li, J.M., 2012. *Sensors* 12, 1181-1193.

611 Hu, K., Liu, J.W., Chen, J., Huang, Y., Zhao, S.L., Tian, J.N., Zhang, G.H., 2013. *Biosens. Bioelectron.*  
612 42, 598-602.

613 Hu, P., Zhu, C.Z., Jin, L.H., Dong, S.J., 2012. *Biosens. Bioelectron.* 34, 83-87.

614 Huang, P.J.J., Kempaiah, R., Liu, J.W., 2011. *J. Mater. Chem.* 21, 8991-8993.

615 Huang, X., Qi, X.Y., Boey, F., Zhang, H., 2012. *Chem. Soc. Rev.* 41, 666-686.

616 Huang, X., Zeng, Z.Y., Zhang, H., 2013. *Chem. Soc. Rev.* 42, 1934-1946.

617 Jiang, B.Y., Wang, M., Chen, Y., Xie, J.Q., Xiang, Y., 2012a. *Biosens. Bioelectron.* 32, 305-308.

618 Jiang, L.P., Yuan, R., Chai, Y.Q., Yuan, Y.L., Bai, L.J., Wang, Y., 2012b. *Analyst* 137, 2415-2420.

619 Jin, G.X., Lu, L.J., Gao, X.Y., Li, M.J., Qiu, B., Lin, Z.Y., Yang, H.H., Chen, G.N., 2013. *Electrochim.*  
620 *Acta* 89, 13-17.

621 Jung, Y.K., Lee, T., Shin, E., Kim, B.S., 2013. *Sci. Rep.* 3, 3367.

622 Kim, D.J., Park, H.C., Sohn, I.Y., Jung, J.H., Yoon, O.J., Park, J.S., Yoon, M.Y., Lee, N.E., 2013. *Small*  
623 9, 3352-3360.

624 Kong, N., Huang, X.D., Cui, L., Liu, J.Q., 2013. *Sci. Adv. Mater.* 5, 1083-1089.

625 Koski, K.J., Cui, Y., 2013. *ACS Nano* 7, 3739-3743.

626 Kuila, T., Bose, S., Khanra, P., Mishra, A.K., Kim, N.H., Lee, J.H., 2011. *Biosens. Bioelectron.* 26,  
627 4637-4648.

628 Kwon, O.S., Park, S.J., Hong, J.Y., Han, A.R., Lee, J.S., Lee, J.S., Oh, J.H., Jang, J., 2012. *ACS Nano* 6,  
629 1486-1493.

630 Leonard, F., Talin, A.A., 2011. *Nat. Nanotechnol.* 6, 773-783.

631 Li, D., Song, S.P., Fan, C.H., 2010. *Acc. Chem. Res.* 43, 631-641.

632 Li, M., Zhou, X.J., Ding, W.Q., Guo, S.W., Wu, N.Q., 2013a. *Biosens. Bioelectron.* 41, 889-893.

633 Li, M., Zhou, X.J., Guo, S.W., Wu, N.Q., 2013b. *Biosens. Bioelectron.* 43, 69-74.

634 Li, X.M., Song, J., Wang, Y., Cheng, T., 2013c. *Anal. Chim. Acta* 797, 95-101.

635 Liang, J.F., Chen, Z.B., Guo, L., Li, L.D., 2011. *Chem. Commun.* 47, 5476-5478.

636 Liang, J.F., Wei, R., He, S., Liu, Y.K., Guo, L., Li, L.D., 2013. *Analyst* 138, 1726-1732.

637 Liao, Y.H., Yuan, R., Chai, Y.Q., Mao, L., Zhuo, Y., Yuan, Y.L., Bai, L.J., Yuan, S.R., 2011. *Sens.*  
638 *Actuators, B* 158, 393-399.

639 Lim, Y.C., Kouzani, A.Z., Duan, W., 2010. *J. Biomed. Nanotechnol.* 6, 93-105.

640 Liu, B.W., Sun, Z.Y., Zhang, X., Liu, J.W., 2013a. *Anal. Chem.* 85, 7987-7993.

641 Liu, F., Zhang, Y., Yu, J.H., Wang, S.W., Ge, S.G., Song, X.R., 2014. *Biosens. Bioelectron.* 51,  
642 413-420.

643 Liu, J.H., Wang, C.Y., Jiang, Y., Hu, Y.P., Li, J.S., Yang, S., Li, Y.H., Yang, R.H., Tan, W.H., Huang,  
644 C.Z., 2013b. *Anal. Chem.* 85, 1424-1430.

645 Liu, J.W., Cao, Z.H., Lu, Y., 2009. *Chem. Rev.* 109, 1948-1998.

646 Liu, Q.Y., Xu, X.J., Zhang, L.N., Luo, X.D., Liang, Y., 2013c. *Analyst* 138, 2661-2668.

647 Liu, S., Xing, X.R., Yu, J.H., Lian, W.J., Li, J., Cui, M., Huang, J.D., 2012a. *Biosens. Bioelectron.* 36,  
648 186-191.

649 Liu, Y.X., Dong, X.C., Chen, P., 2012b. *Chem. Soc. Rev.* 41, 2283-2307.

650 Loo, A.H., Bonanni, A., Pumera, M., 2012. *Nanoscale* 4, 143-147.

651 Loo, A.H., Bonanni, A., Pumera, M., 2013a. *Chem. Asian J.* 8, 198-203.

652 Loo, A.H., Bonanni, A., Pumera, M., 2013b. *Nanoscale* 5, 4758-4762.

653 Lu, C.H., Li, J.A., Lin, M.H., Wang, Y.W., Yang, H.H., Chen, X., Chen, G.N., 2010. *Angew. Chem. Int.*  
654 *Ed.* 49, 8454-8457.

655 Lu, J.J., Yan, M., Ge, L., Ge, S.G., Wang, S.W., Yan, J.X., Yu, J.H., 2013. *Biosens. Bioelectron.* 47,  
656 271-277.

657 Lubin, A.A., Plaxco, K.W., 2010. *Acc. Chem. Res.* 43, 496-505.

658 Maiti, U.N., Lee, W.J., Lee, J.M., Oh, Y., Kim, J.Y., Kim, J.E., Shim, J., Han, T.H., Kim, S.O., 2014.  
659 *Adv. Mater.* 26, 40-67.

660 Mao, H.Y., Laurent, S., Chen, W., Akhavan, O., Imani, M., Ashkarran, A.A., Mahmoudi, M., 2013.  
661 *Chem. Rev.* 113, 3407-3424.

662 Meir, A., Stojanovic, M., Marks, R.S., 2007. *Aptameric Biosensors*, in: Marks, R.S., Cullen, D., Lowe,  
663 C., Weetall H.H., Karube I., (Eds), *Handbook of Biosensors and Biochips*. John Wiley & Sons  
664 Ltd Publishers, pp. 217-232.

665 Novoselov, K.S., Geim, A.K., Morozov, S.V., Jiang, D., Zhang, Y., Dubonos, S.V., Grigorieva, I.V.,  
666 Firsov, A.A., 2004. *Science* 306, 666-669.

667 Ohno, Y., Maehashi, K., Inoue, K., Matsumoto, K., 2011. *Jpn. J. Appl. Phys.* 50, 070120.

668 Ohno, Y., Maehashi, K., Matsumoto, K., 2010. *J. Am. Chem. Soc.* 132, 18012-18013.

669 Park, J.W., Lee, S.J., Choi, E.J., Kim, J., Song, J.Y., Gu, M.B., 2014. *Biosens. Bioelectron.* 51,  
670 324-329.

671 Park, J.W., Tatavarty, R., Kim, D.W., Jung, H.T., Gu, M.B., 2012. *Chem. Commun.* 48, 2071-2073.  
672 Park, S., Ruoff, R.S., 2009. *Nat. Nanotechnol.* 4, 217-224.  
673 Patel, D.J., Suri, A.K., Jiang, F., Jiang, L.C., Fan, P., Kumar, R.A., Nonin, S., 1997. *J. Mol. Biol.* 272,  
674 645-664.  
675 Peng, K.F., Zhao, H.W., Wu, X.F., Yuan, Y.L., Yuan, R., 2012. *Sens. Actuators, B* 169, 88-95.  
676 Ping, J.F., Wang, Y.X., Fan, K., Wu, J., Ying, Y.B., 2011. *Biosens. Bioelectron.* 28, 204-209.  
677 Ping, J.F., Wu, J., Wang, Y.X., Ying, Y.B., 2012. *Biosens. Bioelectron.* 34, 70-76.  
678 Pu, W.D., Zhang, L., Huang, C.Z., 2012. *Anal. Methods* 4, 1662-1666.  
679 Pu, Y., Zhu, Z., Han, D., Liu, H.X., Liu, J., Liao, J., Zhang, K.J., Tan, W.H., 2011. *Analyst* 136,  
680 4138-4140.  
681 Qi, C., Bing, T., Mei, H.C., Yang, X.J., Liu, X.J., Shangguan, D.H., 2013. *Biosens. Bioelectron.* 41,  
682 157-162.  
683 Qin, H.X., Liu, J.Y., Chen, C.G., Wang, J.H., Wang, E.K., 2012. *Anal. Chim. Acta* 712, 127-131.  
684 Qiu, L., Zhou, H., Zhu, W.P., Qiu, L.P., Jiang, J.H., Shen, G.L., Yu, R.Q., 2013. *New J. Chem.* 37,  
685 3998-4003.  
686 Rao, C.N.R., Sood, A.K., Subrahmanyam, K.S., Govindaraj, A., 2009. *Angew. Chem. Int. Ed.* 48,  
687 7752-7777.  
688 Robertson, D.L., Joyce, G.F., 1990. *Nature* 344, 467-468.  
689 Sheng, L.F., Ren, J.T., Miao, Y.Q., Wang, J.H., Wang, E.K., 2011. *Biosens. Bioelectron.* 26, 3494-3499.  
690 Shi, Y., Dai, H.C., Sun, Y.J., Hu, J.T., Ni, P.J., Li, Z., 2013. *Analyst* 138, 7152-7156.  
691 Song, S.P., Wang, L.H., Li, J., Zhao, J.L., Fan, C.H., 2008. *Trends Anal. Chem.* 27, 108-117.  
692 Song, W., Li, H., Liu, H.P., Wu, Z.S., Qiang, W.B., Xu, D.K., 2013. *Electrochem. Commun.* 31, 16-19.  
693 Song, Y.H., Yang, X., Li, Z.Q., Zhao, Y.J., Fan, A.P., 2014. *Biosens. Bioelectron.* 51, 232-237.  
694 Subramanian, P., Lesniewski, A., Kaminska, I., Vlandas, A., Vasilescu, A., Niedziolka-Jonsson, J.,  
695 Pichonat, E., Happy, H., Boukherroub, R., Szunerits, S., 2013. *Biosens. Bioelectron.* 50,  
696 239-243.  
697 Sun, T., Wang, L., Li, N., Gan, X.X., 2011a. *Bioprocess Biosyst. Eng.* 34, 1081-1085.  
698 Sun, W.L., Shi, S., Yao, T.M., 2011b. *Anal. Methods* 3, 2472-2474.  
699 Sun, Y.B., Yang, S.B., Zhao, G.X., Wang, Q., Wang, X.K., 2013. *Chem. Asian J.* 8, 2755-2761.  
700 Tang, D.P., Tang, J., Li, Q.F., Liu, B.Q., Yang, H.H., Chen, G.N., 2011a. *RSC Adv.* 1, 40-43.  
701 Tang, D.P., Tang, J., Li, Q.F., Su, B.L., Chen, G.N., 2011b. *Anal. Chem.* 83, 7255-7259.  
702 Tuerk, C., Gold, L., 1990. *Science* 249, 505-510.  
703 Ueno, Y., Furukawa, K., Matsuo, K., Inoue, S., Hayashi, K., Hibino, H., 2013. *Chem. Commun.* 49,  
704 10346-10348.  
705 Vinkenborg, J.L., Karnowski, N., Famulok, M., 2011. *Nat. Chem. Biol.* 7, 519-527.  
706 Wang, G.Q., Wang, Y.Q., Chen, L.X., Choo, J., 2010a. *Biosens. Bioelectron.* 25, 1859-1868.  
707 Wang, L., Xu, M., Han, L., Zhou, M., Zhu, C.Z., Dong, S.J., 2012a. *Anal. Chem.* 84, 7301-7307.

708 Wang, L., Zhu, C.Z., Han, L., Jin, L.H., Zhou, M., Dong, S.J., 2011a. *Chem. Commun.* 47, 7794-7796.  
709 Wang, L., Zhu, J.B., Han, L., Jin, L.H., Zhu, C.Z., Wang, E.K., Dong, S.J., 2012b. *ACS Nano* 6,  
710 6659-6666.  
711 Wang, Q.B., Wang, W., Lei, J.P., Xu, N., Gao, F.L., Ju, H.X., 2013a. *Anal. Chem.* 85, 12182-12188.  
712 Wang, Q.H., Kalantar-Zadeh, K., Kis, A., Coleman, J.N., Strano, M.S., 2012c. *Nat. Nanotechnol.* 7,  
713 699-712.  
714 Wang, R.E., Zhang, Y., Cai, J., Cai, W., Gao, T., 2011b. *Curr. Med. Chem.* 18, 4175-4184.  
715 Wang, S.E., Si, S.H., 2013. *Appl. Spectrosc.* 67, 1270-1274.  
716 Wang, X.Y., Gao, A., Lu, C.C., He, X.W., Yin, X.B., 2013b. *Biosens. Bioelectron.* 48, 120-125.  
717 Wang, Y., Li, Z.H., Hu, D.H., Lin, C.T., Li, J.H., Lin, Y.H., 2010b. *J. Am. Chem. Soc.* 132, 9274-9276.  
718 Wang, Y., Yuan, R., Chai, Y.Q., Yuan, Y.L., Bai, L.J., 2012d. *Biosens. Bioelectron.* 38, 50-54.  
719 Wang, Y., Yuan, R., Chai, Y.Q., Yuan, Y.L., Bai, L.J., Liao, Y.H., 2011c. *Biosens. Bioelectron.* 30,  
720 61-66.  
721 Wang, Y.P., Xiao, Y.H., Ma, X.L., Lia, N., Yang, X.D., 2012e. *Chem. Commun.* 48, 738-740.  
722 Wang, Y.X., Ye, Z.Z., Si, C.Y., Ying, Y.B., 2012f. *Chin. J. Anal. Chem.* 40, 634-642.  
723 Wei, W., Li, D.F., Pan, X.H., Liu, S.Q., 2012. *Analyst* 137, 2101-2106.  
724 Wen, Y.Q., Li, F.B.Y., Dong, X.C., Zhang, J., Xiong, Q.H., Chen, P., 2013. *Adv. Healthcare Mater.* 2,  
725 271-274.  
726 Willner, I., Zayats, M., 2007. *Angew. Chem. Int. Ed.* 46, 6408-6418.  
727 Wu, J.S., Pisula, W., Mullen, K., 2007. *Chem. Rev.* 107, 718-747.  
728 Wu, S.J., Duan, N., Ma, X.Y., Xia, Y., Wang, H.G., Wang, Z.P., Zhang, Q., 2012. *Anal. Chem.* 84,  
729 6263-6270.  
730 Xiao, Y.H., Wang, Y.P., Wu, M., Ma, X.L., Yang, X.D., 2013. *J. Electroanal. Chem.* 702, 49-55.  
731 Xie, L.L., You, L.Q., Cao, X.Y., 2013. *Spectrochim. Acta, Part A* 109, 110-115.  
732 Xie, S.B., Chai, Y.Q., Yuan, R., Bai, L.J., Yuan, Y.L., Wang, Y., 2012a. *Anal. Chim. Acta* 755, 46-53.  
733 Xie, S.B., Yuan, R., Chai, Y.Q., Bai, L.J., Yuan, Y.L., Wang, Y., 2012b. *Talanta* 98, 7-13.  
734 Xing, X.J., Liu, X.G., Yue, H., Luo, Q.Y., Tang, H.W., Pang, D.W., 2012. *Biosens. Bioelectron.* 37,  
735 61-67.  
736 Xu, M.S., Liang, T., Shi, M.M., Chen, H.Z., 2013a. *Chem. Rev.* 113, 3766-3798.  
737 Xu, Z.H., He, C., Sun, T., Wang, L., 2013b. *Electroanalysis* 25, 2339-2344.  
738 Yan, G.P., Wang, Y.H., He, X.X., Wang, K.M., Liu, J.Q., Du, Y.D., 2013a. *Biosens. Bioelectron.* 44,  
739 57-63.  
740 Yan, M., Sun, G.Q., Liu, F., Lu, J.J., Yu, J.H., Song, X.R., 2013b. *Anal. Chim. Acta* 798, 33-39.  
741 Yang, W.R., Ratnac, K.R., Ringer, S.P., Thordarson, P., Gooding, J.J., Braet, F., 2010. *Angew. Chem.*  
742 *Int. Ed.* 49, 2114-2138.  
743 Yu, Y., Liu, Y., Zhen, S.J., Huang, C.Z., 2013a. *Chem. Commun.* 49, 1942-1944.  
744 Yu, Y.Q., Cao, Q., Zhou, M., Cui, H., 2013b. *Biosens. Bioelectron.* 43, 137-142.

745 Yuan, Y.L., Gou, X.X., Yuan, R., Chai, Y.Q., Zhuo, Y., Mao, L., Gan, X.X., 2011a. *Biosens. Bioelectron.*  
746 26, 4236-4240.

747 Yuan, Y.L., Gou, X.X., Yuan, R., Chai, Y.Q., Zhuo, Y., Ye, Y., Gan, X.X., 2011b. *Biosens. Bioelectron.*  
748 30, 123-127.

749 Yuan, Y.L., Liu, G.P., Yuan, R., Chai, Y.Q., Gan, X.X., Bai, L.J., 2013. *Biosens. Bioelectron.* 42,  
750 474-480.

751 Yuan, Y.X., Wu, S.F., Shu, F., Liu, Z.H., 2014. *Chem. Commun.* 50, 1095-1097.

752 Zhang, D.D., Fu, L., Liao, L., Liu, N., Dai, B.Y., Zhang, C.X., 2012a. *Nano Res.* 5, 875-887.

753 Zhang, D.P., Lu, M.L., Wang, H.L., 2011a. *J. Am. Chem. Soc.* 133, 9188-9191.

754 Zhang, H.F., Han, Y.J., Guo, Y.J., Dong, C., 2012b. *J. Mater. Chem.* 22, 23900-23905.

755 Zhang, J., Chai, Y.Q., Yuan, R., Yuan, Y.L., Bai, L.J., Xie, S.B., 2013a. *Analyst* 138, 6938-6945.

756 Zhang, J.N., Liu, B., Liu, H.X., Zhang, X.B., Tan, W.H., 2013b. *Nanomedicine* 8, 983-993.

757 Zhang, P., Wang, Y., Leng, F., Xiong, Z.H., Huang, C.Z., 2013c. *Talanta* 112, 117-122.

758 Zhang, X.R., Li, S.G., Jin, X., Zhang, S.S., 2011b. *Chem. Commun.* 47, 4929-4931.

759 Zhang, Z., Luo, L.Q., Zhu, L.M., Ding, Y.P., Deng, D.M., Wang, Z.X., 2013d. *Analyst* 138, 5365-5370.

760 Zhang, Z.H., Liu, S.L., Shi, Y., Zhang, Y.C., Peacock, D., Yan, F.F., Wang, P.Y., He, L.H., Feng, X.Z.,  
761 Fang, S.M., 2014. *J. Mater. Chem. B* 2, 1530-1538.

762 Zhao, J., Chen, G.F., Zhu, L., Li, G.X., 2011. *Electrochem. Commun.* 13, 31-33.

763 Zheng, T.T., Tan, T.T., Zhang, Q.F., Fu, J.J., Wu, J.J., Zhang, K., Zhu, J.J., Wang, H., 2013. *Nanoscale* 5,  
764 10360-10368.

765 Zhou, H., Zhang, Y.Y., Liu, J., Xu, J.J., Chen, H.Y., 2013. *Chem. Commun.* 49, 2246-2248.

766 Zhou, J., Battig, M.R., Wang, Y., 2010. *Anal. Bioanal. Chem.* 398, 2471-2480.

767 Zhu, C.F., Zeng, Z.Y., Li, H., Li, F., Fan, C.H., Zhang, H., 2013a. *J. Am. Chem. Soc.* 135, 5998-6001.

768 Zhu, W.P., Zhao, Z.W., Li, Z., Li, H., Jiang, J.H., Shen, G.L., Yu, R.Q., 2013b. *New J. Chem.* 37,  
769 927-932.

770 Zhuang, H.L., Zhen, S.J., Wang, J., Huang, C.Z., 2013. *Anal. Methods* 5, 208-212.

771 Zuo, P., Li, X.J., Dominguez, D.C., Ye, B.C., 2013. *Lab Chip* 13, 3921-3928.

772

## 774 Graphene-based transducers for electrochemical aptasensors.

Analyte	Transducer	Signal molecule	Immobilization method for aptamer	Electrochemical technique	Linear range	Detection limit	Ref.
<b>Label</b>							
ATP	MGNs	Fc	Physical adsorption	SWV	$1.0 \times 10^{-3}$ - 300 $\mu$ M	$0.1 \times 10^{-3}$ pM	(Tang et al., 2011a)
ATP	MGNs	Fc	Physical adsorption	SWV	$1.0 \times 10^{-6}$ - 500 $\mu$ M	0.1 pM	(Tang et al., 2011b)
Cocaine		Th			$1.0 \times 10^{-5}$ - 400 $\mu$ M	1.5 pM	
Cocaine	GNs/AuNPs	<i>p</i> -APP (AP)	Au-S	DPV	$1.0 \times 10^{-3}$ - 0.5 $\mu$ M	$1.0 \times 10^{-3}$ pM	(Jiang et al., 2012a)
L-histidine	GNs-AuNPs	Fc	Au-S	SWV	$1.0 \times 10^{-5}$ - 10 $\mu$ M	0.1 pM	(Liang et al., 2011)
HL-60 cell	GNs-AuNPs	Aq	Au-S	DPV	$5 \times 10^2$ - $1 \times 10^7$ cells/mL	350 cells/mL	(Zheng et al., 2013)
CEM cell		Th					
Thrombin	GNs-PTCDA/AuNPs	H <sub>2</sub> O <sub>2</sub> (HRP)	Au-S	CA	$1.0 \times 10^{-6}$ - 1.0 nM	$0.65 \times 10^{-3}$ pM	(Peng et al., 2012)
Thrombin	GNs-PANI-AuNPs	GOD	Au-S	CV	$1.0 \times 10^{-3}$ - 30 nM	0.56 pM	(Bai et al., 2013)
Thrombin	GNs-SWCNTs/AuNPs/NiHCF NPs/AuNPs	H <sub>2</sub> O <sub>2</sub> (HRP)	Au-S	DPV	$1.0 \times 10^{-2}$ - 50 nM	2.0 pM	(Yuan et al., 2011a)
Thrombin	GNs-PAMAM	Th	Amide	DPV	$1.0 \times 10^{-4}$ - 80 nM	0.05 pM	(Zhang et al., 2013a)
PDGF	GNs-PDDA-AuNPs	GOD	Au-amino	CV	$5.0 \times 10^{-3}$ - 60 nM	1.7 pM	(Deng et al., 2013)
PDGF	OGNs/AuNPs	AA-P (AP)	Au-amino	DPV	$2.0 \times 10^{-3}$ - 40 nM	0.6 pM	(Han et al., 2013)
<b>Label free</b>							
Thrombin	GQDs	[Fe(CN) <sub>6</sub> ] <sup>3-/4-</sup>	Physical adsorption	DPV	200 - 500 nM	0.1 pM	(Zhao et al., 2011)
Thrombin	GNs-NA/MB/AuNPs	MB	Au-S	DPV	0.01 - 50 nM	6.0 pM	(Sun et al., 2011a)
Thrombin	GNs-PTCA/AuNPs	PTCA	Au-S	DPV	$1.0 \times 10^{-3}$ - 40 nM	0.2 pM	(Yuan et al., 2011b)
Thrombin	GNs-NA-NiHCFNPs/AuNPs	[Fe(CN) <sub>6</sub> ] <sup>3-/4-</sup>	Au-S	CV	$1.0 \times 10^{-3}$ - 1.0 nM	0.3 pM	(Jiang et al., 2012b)
Thrombin	GNs-Tb-AuNPs	Tb	Au-S	CV	$1.0 \times 10^{-3}$ - 80 nM	0.33 pM	(Xie et al., 2012b)
Thrombin	GNs-Th/AuNPs	Th	Au-S	DPV	0.5 - 40 nM	0.093 nM	(Zhang et al., 2013d)
Thrombin	(GNs-PAA/CdSeNPs)	AA	Phosphoramidate	PEC	$1.0 \times 10^{-3}$ - $1.0 \times 10^{-2}$ nM	0.45 pM	(Zhang et al., 2011b)
Thrombin	GNs-CS	[Fe(CN) <sub>6</sub> ] <sup>3-/4-</sup>	Amide	DPV	$1.0 \times 10^{-3}$ - $1.0 \times 10^{-4}$ nM	$0.45 \times 10^{-3}$ pM	(Wang et al., 2012e)
Thrombin					$1.0 \times 10^{-3}$ - 0.4 nM	0.35 pM	
Lysozyme	GNs-Orange II	Orange II	Physical adsorption	DPV	$5.0 \times 10^{-3}$ - 0.7 nM	1.0 pM	(Guo et al., 2013)
Lysozyme	GNs-CS	[Fe(CN) <sub>6</sub> ] <sup>3-/4-</sup>	Amide	EIS	10 - 500 nM	$6.0 \times 10^{-3}$ pM	(Xiao et al., 2013)
Lysozyme	GNs/Fe <sub>2</sub> O <sub>3</sub>	[Fe(CN) <sub>6</sub> ] <sup>3-/4-</sup>	Electrostatic adsorption	EIS	5.0 - $5.0 \times 10^3$ ng/mL	0.16 ng/mL	(Du et al., 2013a)
D-VP	GNs-Polyelectrolyte-MB	MB	Electrostatic adsorption	DPV	1.0 - 265 ng/mL	1.0 ng/mL	(Qin et al., 2012)
D-VP	GNs-MS-AuNPs/PEI-Fc	Fc	Au-S	DPV	$5.0 - 56.5 \times 10^3$ ng/mL	5.0 ng/mL	(Du et al., 2012b)
ATP	GNs-Porphyrin	Porphyrin	Physical adsorption	DPV	$2.2 \times 10^{-3}$ - 1.3 $\mu$ M	0.7 nM	(Zhang et al., 2012b)
Dopamine	GNs-PANI	[Fe(CN) <sub>6</sub> ] <sup>3-/4-</sup>	Phosphoramidate	SWV	$7.0 \times 10^{-3}$ - 90 nM	1.98 pM	(Liu et al., 2012a)
HeLa cell	GNs-PTCA	[Fe(CN) <sub>6</sub> ] <sup>3-/4-</sup>	Amide	EIS	$1.0 \times 10^5$ - $1.0 \times 10^6$ cells/mL	794 cells/mL	(Feng et al., 2011)
SK-BR-3 cell	GNs-ZnO/AuNPs	AA	Au-amino	PEC	$1.0 \times 10^2$ - $1.0 \times 10^6$ cells/mL	58 cells/mL	(Liu et al., 2014)

775 ATP: adenosine triphosphate; MGNs: magnetic graphene nanosheets; Fc: ferrocene; SWV: square wave voltammetry; Th:

776 thionine; GNs: graphene nanosheets; AuNPs: gold nanoparticles; SWCNTs: single-walled carbon nanotubes; NiHCFNPs: nickel

777 hexacyanoferrate nanoparticles; HRP: horseradish peroxidases; DPV: differential pulse voltammetry; *p*-APP: *p*-amino phenyl

778 phosphate; AP: alkaline phosphatase; PTCDA: 3,4,9,10-perylene tetracarboxylic dianhydride; CA: chronoamperometry; PANI:

779 polyaniline; GOD: glucose oxidase; CV: cyclic voltammetry; Aq: anthraquinone; PDGF: platelet-derived growth factor; PDDA:

780 poly(diallyldimethylammonium chloride); OGNs: onion-like mesoporous graphene nanosheets; AA-P: ascorbic acid 2-phosphate;

781 PAMAM: carboxyl-terminated polyamidoamine; GQDs: graphene quantum dots; D-VP: D-vasopressin; MB: methylene blue;

782 EIS: electrochemical impedance spectroscopy; NA: Nafion; PTCA: 3,4,9,10-perylene tetracarboxylic acid; Tb: toluidine blue;

783 MS: mesoporous silica; PEI: poly(ethyleneimine); CS: chitosan; PAA: poly(acrylic acid); AA: ascorbic acid; PEC:

784 photoelectrochemistry.

785 **Table 2**786 **Graphene and its derivatives-based nanocarriers for electrochemical aptasensors.**

Analyte	Nanocarrier	Signal molecule	Electrochemical technique	Linear range	Detection limit	Ref.
<b>Graphene</b>						
Thrombin	GNs-HCoPt-Th-HRP-TBA	H <sub>2</sub> O <sub>2</sub>	DPV	1.0×10 <sup>-3</sup> - 50 nM	0.34 pM	(Wang et al., 2011c)
Thrombin	GNs-PAMMA-Th-TBA-hemin-BSA	NADH	DPV	2.0×10 <sup>-4</sup> - 30 nM	0.1 pM	(Yuan et al., 2013)
Thrombin	GNs-PdNPs-Tb-TBA-hemin-BSA	NADH	DPV	1.0×10 <sup>-4</sup> - 50 nM	0.03 pM	(Xie et al., 2012a)
Thrombin	GNs-PDDA-PtNPs/TBA-GOD	Glucose	DPV	3.0×10 <sup>-4</sup> - 35 nM	0.21 pM	(Bai et al., 2012a)
Thrombin	GNs-Fc-PtNPs-TBA/GOD-HRP	Fc	DPV	0.02 - 45 nM	11.0 pM	(Bai et al., 2012b)
PDGF	GNs-Tb-PtNPs-PBA/GOD-HRP	Tb	DPV	0.01 - 35 nM	8.0 pM	(Bai et al., 2012b)
IgE	GNs-AgNPs-Ab	AgNPs	SWASV	1.0×10 <sup>-2</sup> - 1.0 µg/mL	3.6 ng/mL	(Song et al., 2013)
<b>Graphene oxide</b>						
Thrombin	GONs-(AP-AuNPs) <sub>2</sub> -TBA	AA-P	DPV	8.0×10 <sup>-3</sup> - 15 nM	2.7×10 <sup>-3</sup> pM	(Wang et al., 2012d)
Thrombin	GONs-TBA	H <sub>2</sub> O <sub>2</sub>	DPV	5.0×10 <sup>-4</sup> - 20 nM	0.15 pM	(Xu et al., 2013b)
Thrombin	GONs-MB	MB	DPV	0.028 - 3.7 nM	3.05 pM	(Chen et al., 2013)
ATP				0.1 - 500 nM	29.1 pM	

787 GNs: graphene nanosheets; HCoPt: hollow CoPt bimetal alloy nanoparticles; Th: thionine; HRP: horseradish peroxidases; TBA:

788 thrombin binding aptamer; DPV: differential pulse voltammetry; PAMMA: carboxyl-terminated polyamidoamine; BSA: bovine

789 serum albumin; NADH: nicotinamide adenine dinucleotide; PdNPs: palladium nanoparticles; Tb: toluidine blue; PDDA:

790 poly(diallyldimethylammonium chloride); PtNPs: platinum nanoparticles; GOD: glucose oxidase; IgE: immunoglobulin E;

791 AgNPs: silver nanoparticles; Ab: antibody; SWASV: square wave anodic stripping voltammetry; PDGF: platelet-derived growth

792 factor; PBA: PDGF binding aptamer; Fc: ferrocene; GONs: graphene oxide nanosheets; AP: alkaline phosphatase; AuNPs: gold

793 nanoparticles; AA-P: ascorbic acid 2-phosphate; ATP: adenosine triphosphate; MB: methylene blue.

794

795 **Table 3**

## 796 Graphene oxide as an effective fluorescence nanoquencher in fluorescent aptasensors.

Analyte	Fluorescent reporter	Linear range	Detection limit	Sample	Comments	Ref.
<b>Normal</b>						
ATP	FAM	10 - 2.5×10 <sup>3</sup> μM	-	JB6 cells	First example of using GO-based fluorescent assay for molecule probing in living cells	(Wang et al., 2010b)
ATP	FAM	5.0 - 2500 μM	2.0 μM	Cancer cell	Long range resonance energy transfer	(He et al., 2011)
ATP	FAM	3 - 320 μM	0.45 μM	-	'Turn off' detection mode and a fluorescein-labeled complementary DNA was used as signal reporter	(Pu et al., 2012)
Ochratoxin A	FAM	50 - 500 nM	21.8 nM	Red wine	Poly(vinyl pyrrolidone) coated GO nanosheets to repel physical adsorption of ochratoxin A	(Sheng et al., 2011)
Ochratoxin A	UCNPs-Er	0.05 - 100 ng/mL	0.02 ng/mL	Maize	Multiplexed analysis	(Wu et al., 2012)
Fumonisin B <sub>1</sub>	UCNPs-Tm	0.1 - 500 ng/mL	0.1 ng/mL			
Mucin 1	Cy5	0.04 - 10 μM	28 nM	Serum	'Turn on' detection mode with low background fluorescence	(He et al., 2012b)
PDGF	FAM	0.167 - 1.167 nM	167 pM	Serum	'Turn on' detection mode and high specificity	(Liang et al., 2013)
VEGF	FAM	0.5 - 5.0 nM	0.25 nM	Serum	'Turn on' detection mode and lower detection limit compared to other optical assays	(Wang and Si, 2013)
ADA	FAM	1.54 - 28.6 nM	1.54 nM	Serum	Competitive assay	(Xing et al., 2012)
Zeatin	FAM	3.0 - 50 μM	0.1 μM		No response to the analogs of zeatin	(Qi et al., 2013)
K <sup>+</sup>	Ru <sup>+</sup>	50 - 500 μM	-	-	Label-free and K <sup>+</sup> stabled G-rich ssDNA as aptamer	(Sun et al., 2011b)
S. aureus	Cy3	10 <sup>4</sup> - 10 <sup>6</sup> cfu/mL	800 cfu/mL		Multiplexed analysis using microfluidic biochip	(Zuo et al., 2013)
S. enterica		42.2 - 675 cfu/mL	61 cfu/mL			
Coralyne	TAMRA	10 - 700 nM	-	Urine	Long range resonance energy transfer and cell imaging	(Zhang et al., 2013c)
PrP	TAMRA	10.2 - 78.8 μg/mL	0.309 μg/mL		Long range resonance energy transfer	(Zhuang et al., 2013)
<b>Amplification</b>						
Theophylline	FAM	0.1 - 10 μM	0.1 μM		DNase I and aptazyme	(Li et al., 2013c)
TPP		0.5 - 100 μM	0.5 μM			
Insulin	FAM	-	5.0 nM		DNase I	(Pu et al., 2011)
ATP	FAM	0.1 - 1.0×10 <sup>3</sup> μM	40 nM		DNase I	(Lu et al., 2010)
ATP	FAM	5.0×10 <sup>-3</sup> - 100 μM	1.0 nM		Exo III	(Hu et al., 2012)
ATP	SYBR Green I	1.0×10 <sup>-3</sup> - 0.2 μM	0.2 nM		Exo III and Label-free	(Zhu et al., 2013b)
Lysozyme	FAM	0.125 - 1 μg/mL	0.08 μg/mL		Exo III	(Chen et al., 2012a)
IFN-γ	FAM	3.5×10 <sup>-3</sup> - 1.0 pM	1.5 fM	Plasma	KF Polymerase	(Hu et al., 2013)
Cocaine	SYBR Green I	0.2 - 100 μM	190 nM	Urine	KF Polymerase and Label-free	(Qiu et al., 2013)

797 ATP: adenosine triphosphate; FAM: carboxyfluorescein; Cy5: cyanine-5; PDGF: platelet derived growth factor; VEGF: vascular

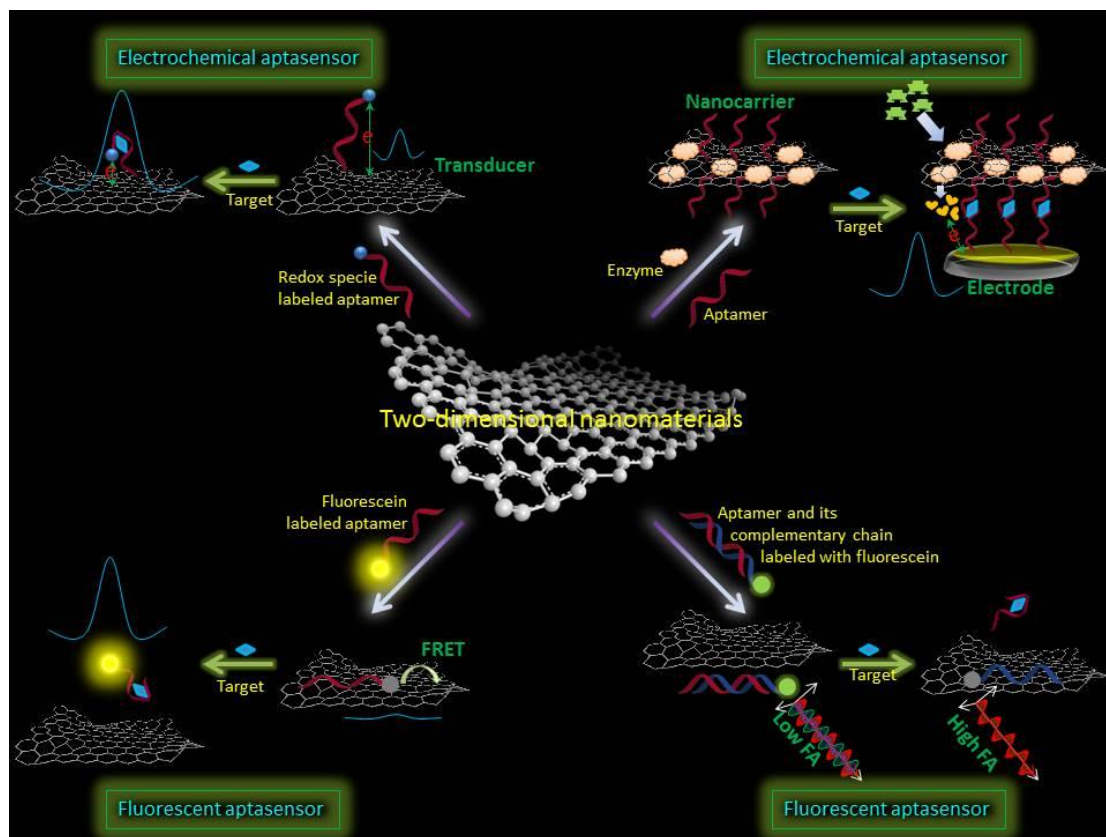
798 endothelial growth factor; ADA: Adenosine deaminase; Ru<sup>+</sup>: Ru polypyridine complex; UCNPs: upconversion fluorescent

799 nanoparticles; S. aureus: Staphylococcus aureus; S. enterica: Salmonella enterica; Cy3: cyanine-3; PrP: cellular prion protein;

800 DNase I: deoxyribonuclease I; TPP: thiamine pyrophosphate; Exo III: exonuclease III; IFN-γ: interferon-gamma; KF polymerase:

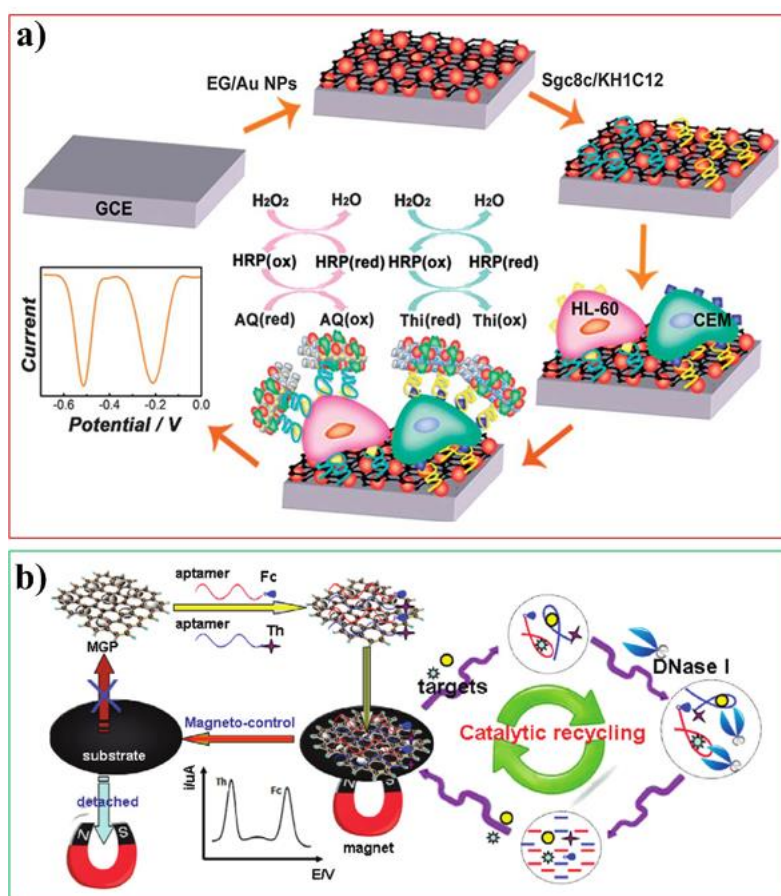
801 Klenow fragment polymerase.

802 **Fig. 1.** Schematic illustration of graphene-like two-dimensional nanomaterials-based  
803 aptasensors.



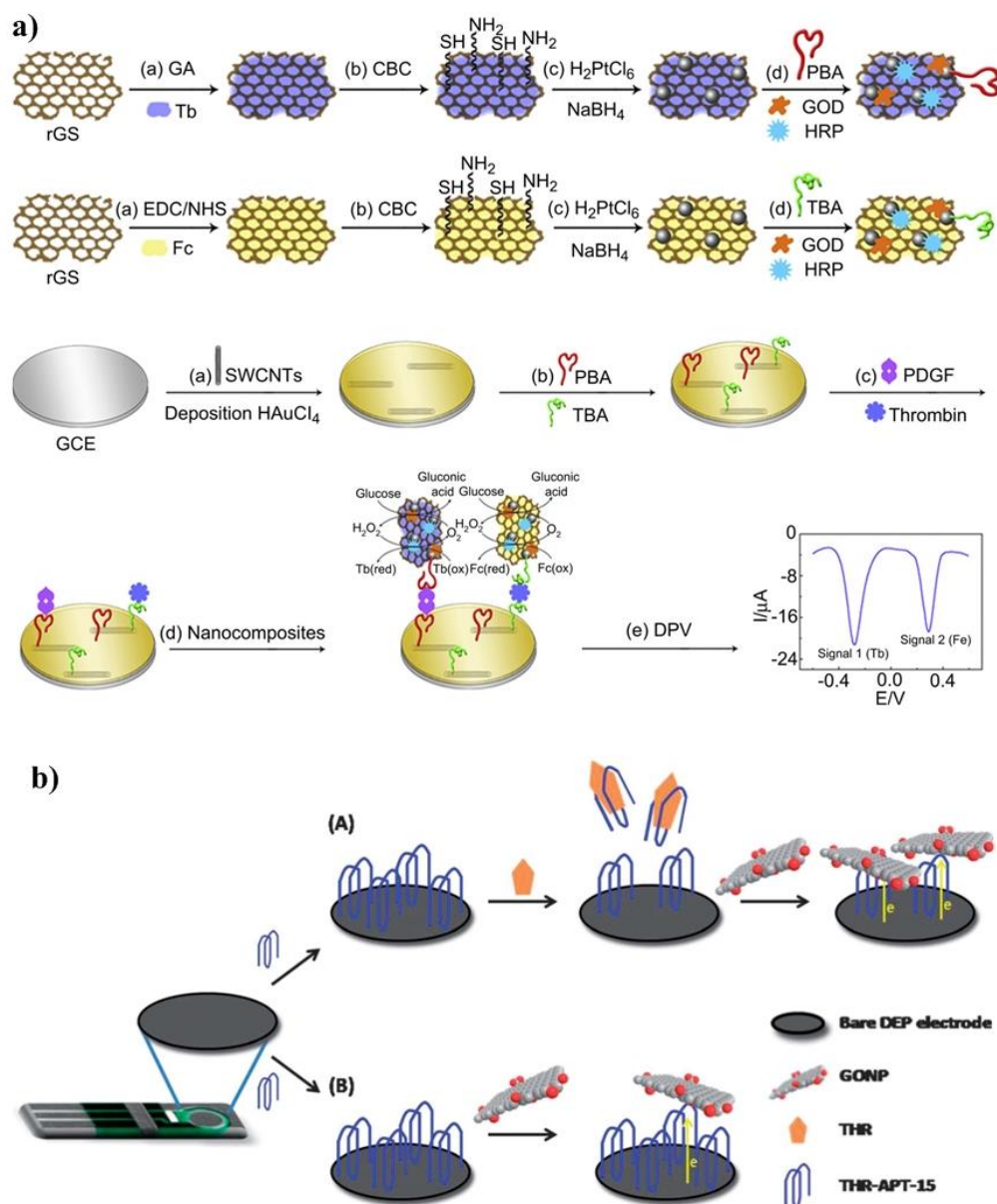
804  
805

806 **Fig. 2.** a) Schematic illustration of the sandwich electrochemical aptasensors for  
 807 simultaneous detection of HL-60 and CEM cells based on a graphene/AuNPs  
 808 platform. Reprinted with permission of The Royal Society of Chemistry from  
 809 reference Zheng et al. (2013). b) Schematic illustration of the multiplexed  
 810 electrochemical aptasensing assay based on magnetic graphene platform and DNase-I  
 811 induced signal amplification. Reprinted with permission of American Chemical  
 812 Society from reference Tang et al. (2011b).



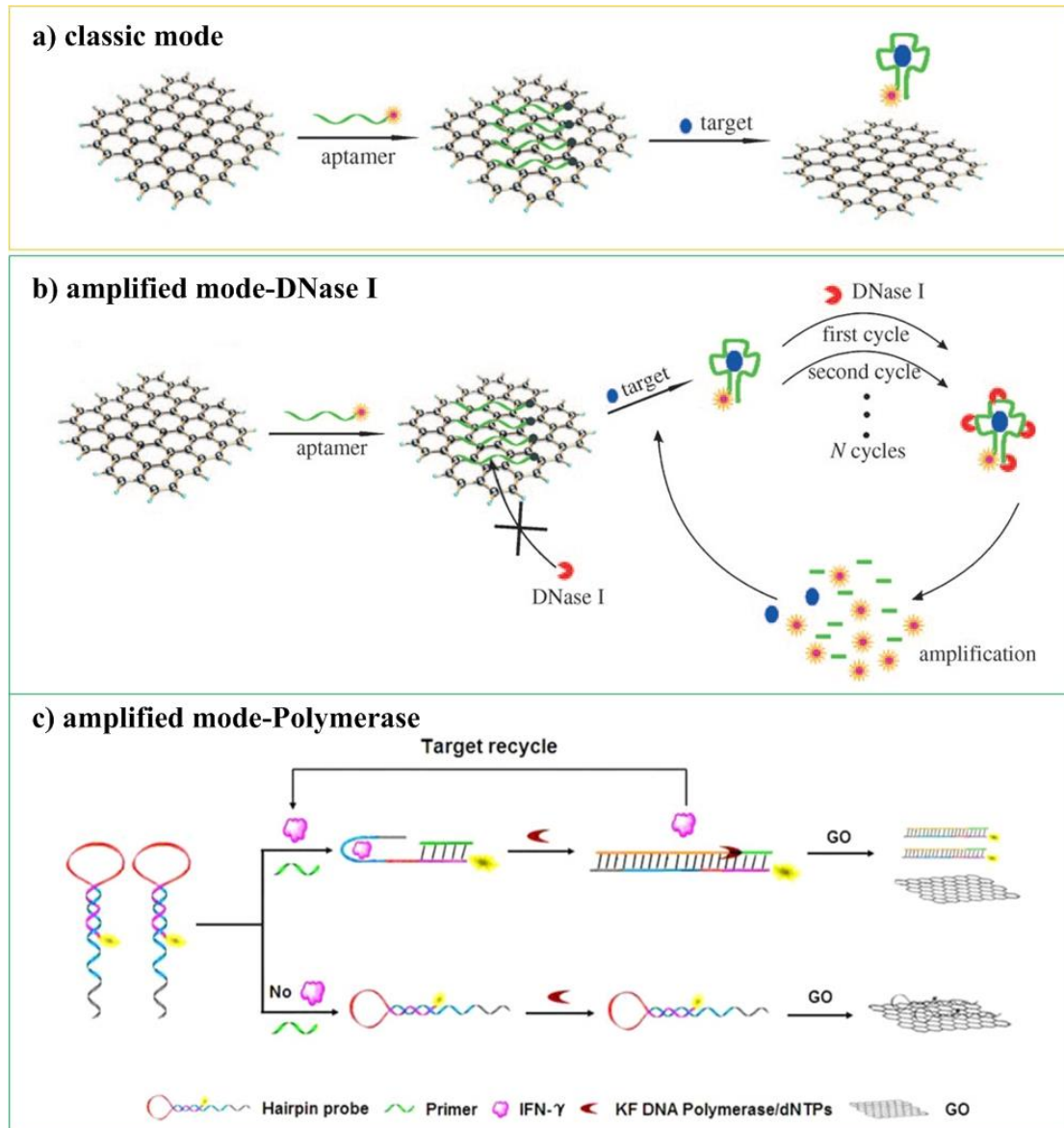
813  
 814

815 **Fig. 3.** a) Fabrication steps for the different graphene-based nanocarriers and the  
 816 sandwich aptasensor. Reprinted with permission of Elsevier from reference Bai et al.  
 817 (2012b). b) Illustration of the utilization of GONPs as inherently electroactive labels  
 818 for thrombin detection. (A) In the presence of THR, the aptamer bound specifically  
 819 to thrombin and resulted in partial removal of immobilized aptamer from the electrode  
 820 surface due to conformational changes. GONPs then adsorbed onto the remaining  
 821 immobilized aptamer due to the strong  $\pi$ - $\pi$  interactions. (B) In the absence of  
 822 thrombin, GONPs were adsorbed onto the immobilized aptamer. Reprinted with  
 823 permission of The Royal Society of Chemistry from reference Loo et al. (2013b).



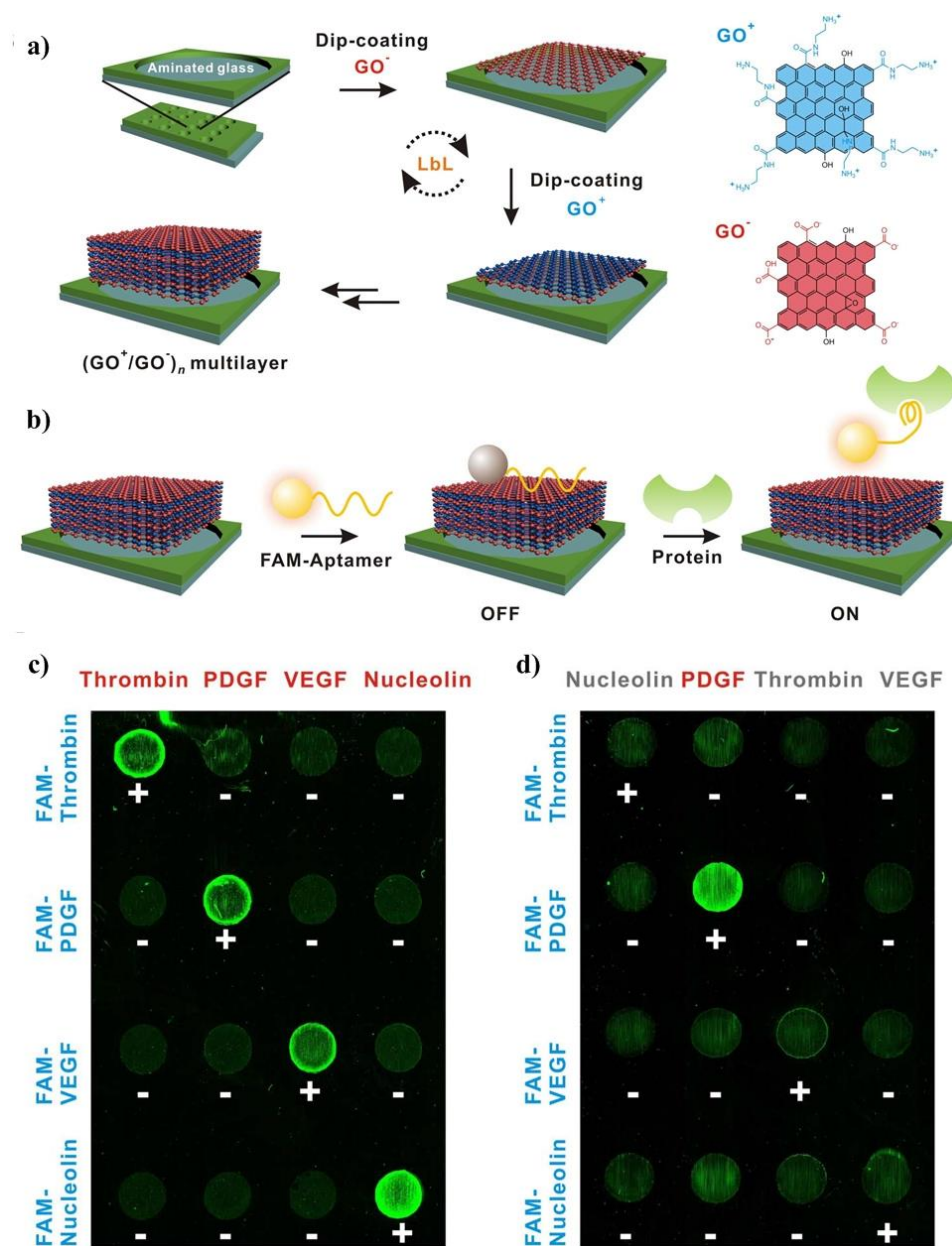
824

825 **Fig. 4.** Illustration of the (a) classic mode, (b) amplified mode-DNase I, and (c)  
 826 amplified mode-polymerase in the GO-based FRET aptasensors. Reprinted with  
 827 permissions of John Wiley & Sons from reference Lu et al. (2010) and Elsevier from  
 828 reference Hu et al. (2013).



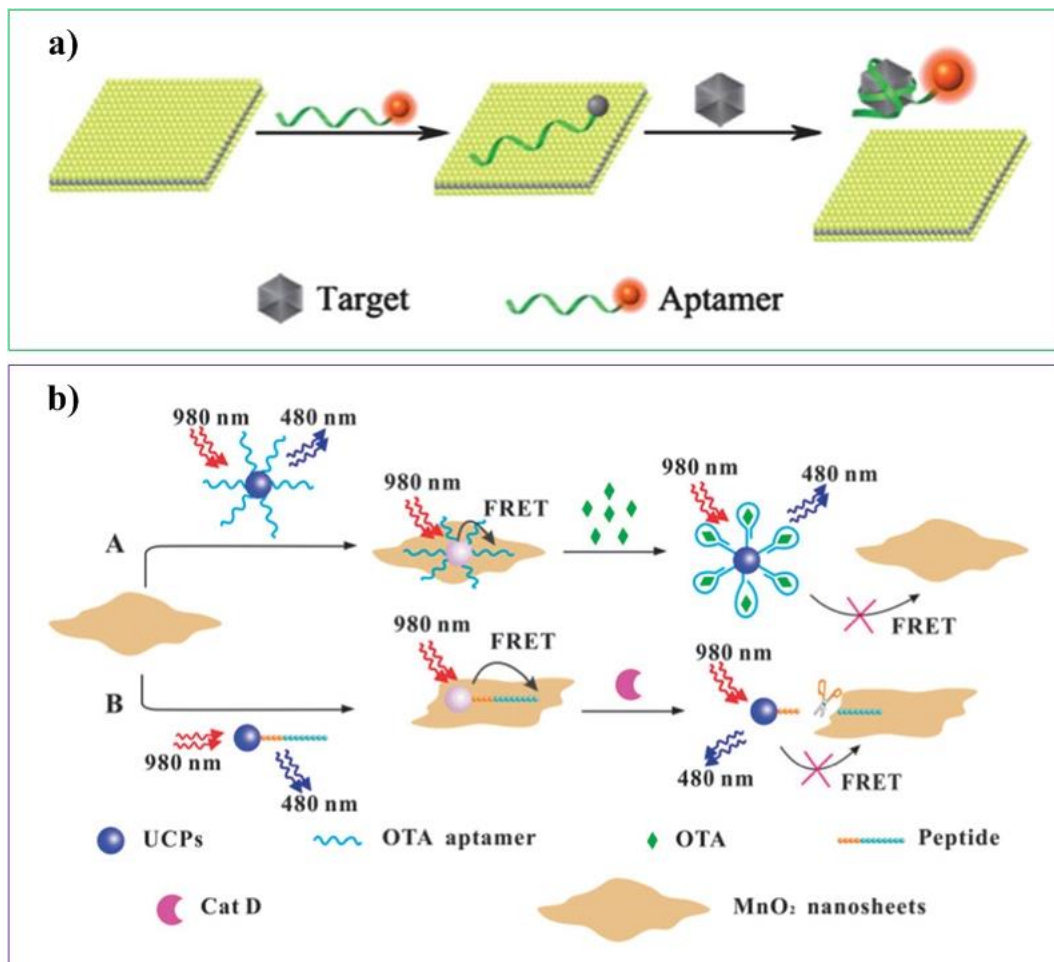
829  
 830

831 **Fig. 5.** Schematic representation of (a) the LbL-assembled GO multilayer array and (b)  
 832 the aptamer-based protein sensing mechanism of the GO multilayer array. (c)  
 833 multiplex detection of four different proteins using their FAM-labeled binding  
 834 aptamers and (d) selective fluorescence recovery of the PDGF aptamer-coated GO  
 835 spot upon PDGF addition. Plus and minus sign respectively indicate the loading and  
 836 unloading of both specific FAM-labeled aptamers and proteins onto the positions.  
 837 Reprinted with permission of Nature Publishing Group from reference Jung et al.  
 838 (2013).



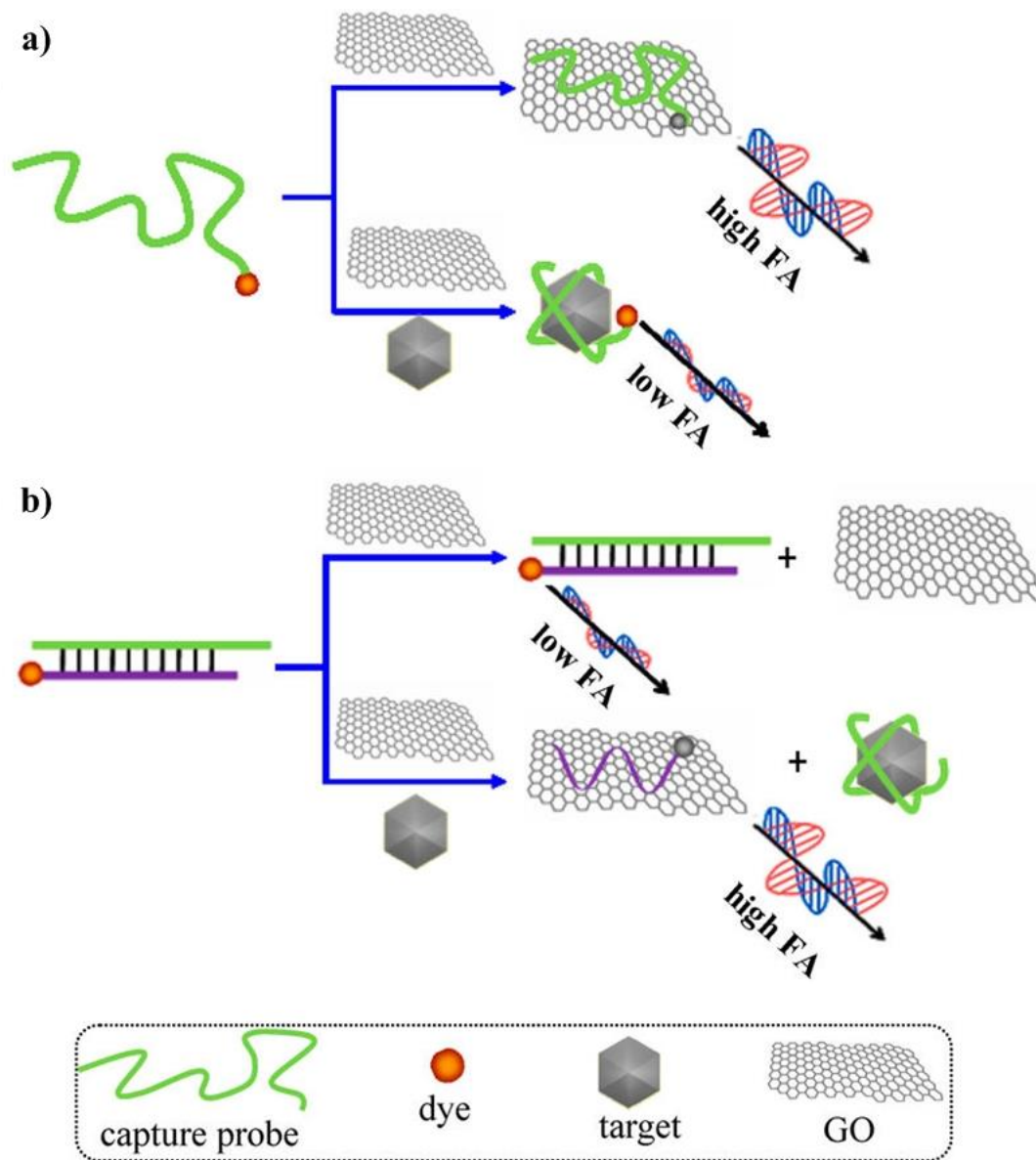
839  
 840

841 **Fig. 6.** Schematic illustration of (a) MoS<sub>2</sub> nanosheets- and (b) MnO<sub>2</sub>  
842 nanosheets-based FRET aptasensors. Reprinted with permissions of The Royal  
843 Society of Chemistry from references Ge et al. (2014) and Yuan et al. (2014).



844  
845

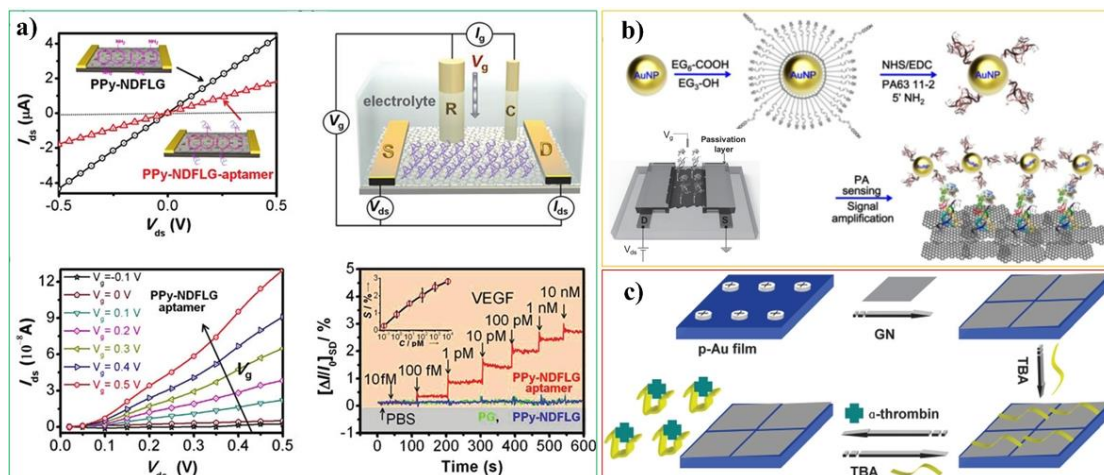
846 **Fig. 7.** General strategies for GO-based signal amplification assay of small molecule  
847 target with (a) FA reduction and (b) FA enhancement detection. Reprinted with  
848 permission of American Chemical Society from reference Liu et al. (2013b).



849

850

851 **Fig. 8.** (a) FET based on polypyrrole-converted nitrogen-doped few-layer graphene as  
 852 channel; (b) Schematic illustration of the use of AuNPs to construct sandwich  
 853 aptasensor based on graphene-based FET; (c) Fabrication steps of graphene-based  
 854 SPR aptasensor. Reprinted with permissions of American Chemical Society from  
 855 reference Kwon et al. (2012), John Wiley & Sons from reference Kim et al. (2013),  
 856 and The Royal Society of Chemistry from reference Wang et al. (2011a).



857  
 858